

# Collectively enhanced ground-state cooling in subwavelength atomic arrays

Oriol Rubies-Bigorda,<sup>1,2,\*</sup> Raphael Holzinger,<sup>3</sup> Ana Asenjo-Garcia,<sup>4</sup> Oriol Romero-Isart,<sup>5,6</sup> Helmut Ritsch,<sup>3</sup> Stefan Ostermann,<sup>2</sup> Carlos Gonzalez-Ballester,<sup>7</sup> Susanne F. Yelin,<sup>2</sup> and Cosimo C. Rusconi<sup>4,†</sup>

<sup>1</sup>*Physics Department, Massachusetts Institute of Technology, Cambridge, Massachusetts 02139, USA*

<sup>2</sup>*Department of Physics, Harvard University, Cambridge, Massachusetts 02138, USA*

<sup>3</sup>*Institute for Theoretical Physics, University of Innsbruck, A-6020 Innsbruck, Austria*

<sup>4</sup>*Department of Physics, Columbia University, New York, New York 10027, USA*

<sup>5</sup>*ICFO - Institut de Ciències Fòniques, The Barcelona Institute of Science and Technology, 08860 Castelldefels (Barcelona), Spain*

<sup>6</sup>*ICREA - Institut Català de Recerca i Estudis Avançats, 08010 Barcelona, Spain*

<sup>7</sup>*Institute for Theoretical Physics, Vienna University of Technology (TU Wien), 1040 Vienna, Austria*

Subwavelength atomic arrays in free space are becoming a leading platform for exploring emergent many-body quantum phenomena. These arrays feature strong light-induced dipole-dipole interactions, resulting in subradiant collective resonances characterized by narrowed linewidths. In this work, we present a sideband cooling scheme for atoms trapped in subwavelength arrays that utilizes these narrow collective resonances. We derive an effective master equation for the atomic motion by adiabatically eliminating the internal degrees of freedom of the atoms, and validate its prediction with numerical simulations of the full system. Our results demonstrate that subradiant resonances enable the cooling of ensembles of atoms to temperatures lower than those achievable without dipole interactions, provided the atoms have different trap frequencies. Remarkably, narrow collective resonances can be sideband-resolved even when the individual atomic transition is not. In such scenarios, ground state cooling becomes feasible solely due to light-induced dipole-dipole interactions. This approach could be utilized for future quantum technologies based on dense ensembles of emitters, and paves the way towards harnessing many-body cooperative decay for enhanced motional control.

Ordered atomic arrays with subwavelength interatomic spacing – i.e., smaller than the characteristic emission wavelength – have emerged as a promising platform to control atom-photon interactions [1]. The optical response of these systems is theoretically well understood in the weak driving limit and when atomic motion is neglected, i.e., when atoms are assumed to be pinned to their respective lattice sites [2, 3]. The combination of dipolar interactions and periodic spatial order causes the atoms to absorb and emit light collectively, leading to the emergence of states with broader (superradiant) and narrower (subradiant) linewidths [4–7]. State-of-the-art cold atom experiments are able to reach the regime where these collective effects play a role and therefore can be probed systematically [8–10]. To fully describe these experiments, however, theory must include effects of atomic recoil and find ways to control and manipulate the motional state of the atoms in the presence of dipolar interactions [11–22]. Previous theoretical work showed that these interactions can cause excess motional heating [18–21], or lead to small reductions of the final atomic temperature of up to 30% [12]. However, the general mechanism that allows or impedes cooling in subwavelength arrays remains unclear.

In this work, we identify two key insights that allow to sideband-cool dipole-interacting atoms trapped in subwavelength arrays to their motional ground state. In laser sideband cooling [23–25], a red detuned motional sideband is resonantly driven to cool a trapped atom to a final motional state temperature proportional to its linewidth. Our first insight is to utilize narrow collective

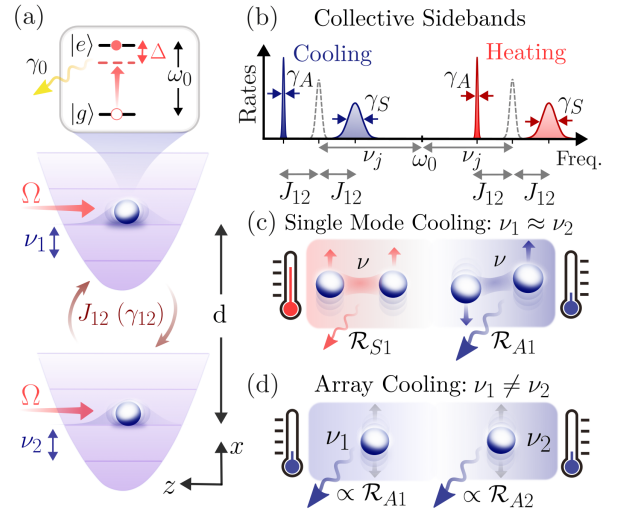


Figure 1. (a) Two harmonically trapped atoms separated by  $d < \lambda_0 = 2\pi c/\omega_0$  are coupled by coherent (dissipative)  $J_{12}$  ( $\gamma_{12}$ ) dipole interactions and are driven by an external laser along the direction of motion ( $z$ ). (b) Motional sidebands: a cooling and a heating sideband is associated to the symmetric (superradiant) and to the antisymmetric (subradiant) transition. The dashed grey lines indicate the sidebands of non-interacting atoms. (c) For  $\nu_1 \approx \nu_2 \approx \nu$ , the center-of-mass (relative) motion of both atoms is independently cooled via the symmetric (antisymmetric) cooling sideband to phonon numbers higher (lower) than that of non-interacting atoms. (d) Lower phonon number per atom can be reached for sufficiently large trap frequency differences, as both atoms are predominantly cooled via the antisymmetric cooling sideband.

sidebands to reduce the final temperature. Notably, collective sidebands can be excited by uniformly driving the array. However, even if the linewidth is reduced, dipole-induced exchange of motional quanta between the atoms leads to an increase of the final temperature. Our second insight is to render these interactions off-resonant by trapping atoms with slightly different trap frequencies. Combining both ideas, we identify the regimes where a subwavelength array of up to a few tens of atoms can be cooled to temperatures lower than in the case of non-interacting atoms.

### System and model

We consider an array of  $N$  two-level atoms ( $|g\rangle, |e\rangle$ ) trapped in a periodic lattice with lattice spacing  $d$ . Each atom  $j$ , with resonance frequency  $\omega_0$  and linewidth  $\gamma_0$ , is harmonically trapped with a site-dependent frequency  $\nu_j$ . We consider motion along one direction. A laser with frequency  $\omega_L$  drives the atomic transition with Rabi frequency  $\Omega$  and induces interactions between the internal (spin) and external (motion) degrees of freedom of the atoms. When  $d \lesssim \lambda_0 = 2\pi c/\omega_0$ , virtual photon exchange processes induce dipole-dipole interactions between atoms affecting both spin and motional degrees of freedom [Fig. 1]. We further assume the motion of each atom to be confined in a region much smaller than  $\lambda_0$ , such that the system is in the Lamb-Dicke regime  $\eta_j \equiv \sqrt{\nu_R/\nu_j} \ll 1$  with  $\nu_R = \hbar\omega_0^2/2mc^2$  the atomic recoil frequency. In what follows, we consider small changes in the trap frequencies such that  $\eta_j \approx \eta$ . In the weak spin-motion coupling regime, i.e., for laser intensities such that  $\eta\Omega$  is smaller than the narrowest sub-radiant collective linewidth, we derive an effective master equation for the atomic motion only. Note that, for trapped atoms, the subradiant linewidth is bounded by  $\gamma_d \gtrsim \eta^2\gamma_0$  [15, 26]. In the frame rotating at the trap frequencies, the master equation reads [27]

$$\begin{aligned} \frac{d}{dt}\hat{\rho}_M = & -i \left[ \sum_{ij} V_{ij} e^{i(\nu_i - \nu_j)t} \hat{b}_i^\dagger \hat{b}_j, \hat{\rho}_M \right] \\ & + \sum_{i,j=1}^N \mathcal{R}_{ij}^- e^{i(\nu_i - \nu_j)t} \left( \hat{b}_j \hat{\rho}_M \hat{b}_i^\dagger - \frac{1}{2} \{ \hat{b}_i^\dagger \hat{b}_j, \hat{\rho}_M \} \right) \\ & + \sum_{i,j=1}^N \mathcal{R}_{ij}^+ e^{-i(\nu_i - \nu_j)t} \left( \hat{b}_i^\dagger \hat{\rho}_M \hat{b}_j - \frac{1}{2} \{ \hat{b}_i \hat{b}_j^\dagger, \hat{\rho}_M \} \right), \end{aligned} \quad (1)$$

where  $\hat{b}_i$  is the motional lowering operator of atom  $i$  along the direction of motion. The coherent  $V_{ij}$  and dissipative  $\mathcal{R}_{ij}^\pm$  coupling rates for  $i \neq j$  are a consequence of dipolar interactions and are given in the Appendix. The second and third terms describe collective cooling and heating processes, respectively. We will compare our analytical

findings to numerical solutions of the full model which explicitly includes both the internal and external degrees of freedom in the Lamb-Dicke limit (see Appendix).

### Non-interacting atoms

When dipole interactions are negligible (that is for  $d \gg \lambda_0$ ), Eq. (1) reduces to the well known laser sideband cooling master equation for each individual atom [25, 28]. Defining the detuning of the laser drive from the atomic resonance as  $\Delta = \omega_L - \omega_0$ , the rates in Eq. (1) read

$$\mathcal{R}_{jj}^\pm = \frac{\eta^2 \Omega^2 \gamma_0}{(-\Delta \pm \nu_j)^2 + \gamma_0^2/4} + \mathcal{D}_{jj}, \quad (2)$$

and  $\mathcal{R}_{ji}^\pm = 0$  for  $i \neq j$ . The first term in Eq. (2) describes the inelastic scattering of a laser photon by annihilating or creating a phonon. For atoms with identical trap frequencies  $\nu_j = \nu$ , these processes are enhanced when the drive is resonant with the red (or cooling)  $\Delta = -\nu$  and blue (or heating)  $\Delta = \nu$  sidebands, respectively [see Fig. 1(b)]. The rate  $\mathcal{D}_{jj}$  describes the atomic recoil heating [28]. The optimal steady state phonon number  $\bar{n}_{ind}$  is obtained for  $\Delta = -\sqrt{\nu^2 + (\gamma_0/2)^2}$  and is set by the ratio  $\nu/\gamma_0$  [25, 29]. In the resolved sideband regime  $\nu \gg \gamma_0$ , the atoms are ground-state cooled to an optimal steady state phonon number  $\bar{n}_{ind}^{(sc)} \approx 13\gamma_0^2/80\nu^2$  at a rate  $\Gamma_{ind}^{(sc)} \approx 4\eta^2\Omega^2/\gamma_0$ , where we included the contribution of recoil heating [30]. In the Doppler or unresolved cooling regime  $\nu \lesssim \gamma_0$ , atoms can only be cooled to the final phonon number  $\bar{n}_{ind}^{(dc)} \approx 7\gamma_0/(20\nu)$  at a slower rate  $\Gamma_{ind}^{(dc)} \approx 8\eta^2\Omega^2\nu/\gamma_0^2$  [31].

### Two interacting atoms

We now consider two atoms at  $d < \lambda_0/2$  polarized perpendicular to both the direction of motion ( $z$ -axis) and the direction of separation ( $x$ -axis), as illustrated in Fig. 1(a) [see Supplemental Material (SM) [32] for other configurations]. To zeroth order in  $\eta$ , that is ignoring motional effects, the dipole-dipole interactions split the single atomic resonance in two distinct peaks associated to the excitation of the ground state  $|gg\rangle$  to the two collective single excitation states  $|S\rangle = (|ge\rangle + |eg\rangle)/\sqrt{2}$  and  $|A\rangle = (|ge\rangle - |eg\rangle)/\sqrt{2}$  [33, 34]. In particular, the transition to the symmetric (antisymmetric) state  $|S\rangle$  ( $|A\rangle$ ) is a bright (dark) transition with linewidth  $\gamma_S = \gamma_0 + \gamma_{12} > \gamma_0$  ( $\gamma_A = \gamma_0 - \gamma_{12} < \gamma_0$ ) and resonance frequency  $\omega_S \equiv \omega_0 + J_{12}$  ( $\omega_A \equiv \omega_0 - J_{12}$ ). Here,  $J_{12}$  ( $\gamma_{12}$ ) is the coherent (dissipative) dipole-dipole interaction strength between the two atoms. Motional effects arise from the first order Lamb-Dicke corrections of the

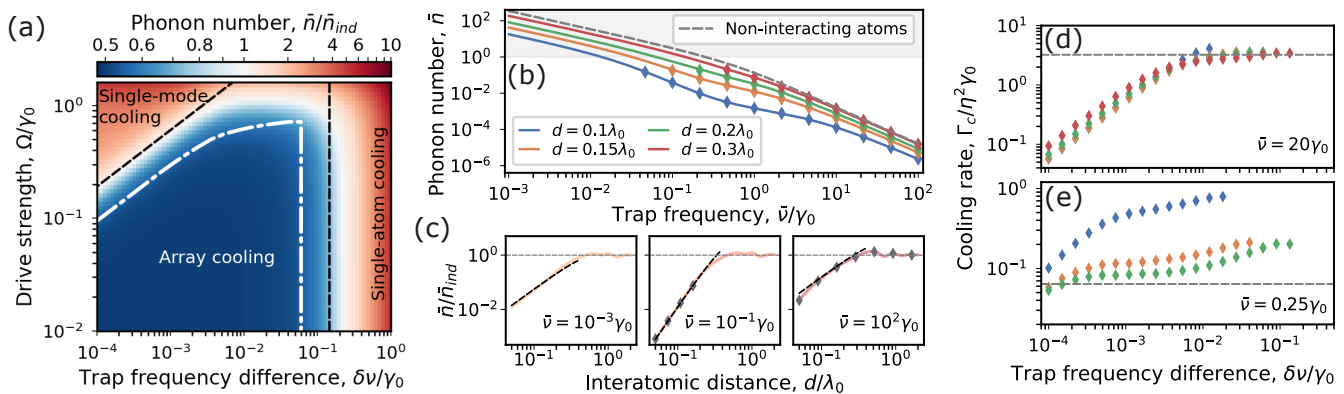


Figure 2. Sideband cooling of two interacting atoms for  $\eta = 0.02$ . (a) Normalized average steady state phonon number,  $\bar{n}/\bar{n}_{ind}$ , as a function of frequency difference  $\delta\nu$  and drive strength  $\Omega$  for  $d = 0.2\lambda_0$ ,  $\nu = 20\gamma_0$  and  $\Delta = -\nu - J_{12}$ , obtained by solving the full system including the spin dynamics. The dashed black lines correspond to the two conditions in Eq. (3), which separate the three cooling regimes. The dash-dotted white line corresponds to the drive strength used to compute the critical cooling rate in panel (d) for  $d = 0.2\lambda_0$ . (b) Average phonon number  $\bar{n}$  as a function of trap frequency  $\nu$  for various atomic separations  $d$  in the array cooling regime with  $\delta\nu = 10^{-3}\gamma_0$ . Enhanced cooling is attained at small separations, when the antisymmetric spin mode becomes subradiant. (c) Scaling of  $\bar{n}$  with  $d$  for various  $\nu$ . The black dashed lines correspond to the analytical estimates given by Eqs. (4-6). (d-e) Critical cooling rate  $\Gamma_c$  as a function of  $\delta\nu$  for various  $d$  and for (d)  $\nu = 20\gamma_0$  and (e)  $\nu = 0.25\gamma_0$ . In panels (b-e), the dashed grey lines correspond to the results for non-interacting atoms, while the solid lines and diamond markers are respectively obtained by solving the effective master equation (1) and the full model including the spin dynamics. Throughout this work, we treat  $\eta$  and  $\nu$  independently to showcase the different cooling regimes that can be reached using different internal transitions or atomic species.

driving Hamiltonian, which excites the cooling and heating sidebands of *both* collective internal transitions illustrated in Fig. 1(b) with strength  $\eta\Omega$ . As a result, the subradiant transition contributes to the cooling process even if, to zeroth order in  $\eta$ , it is not directly excited by the drive. The rates in Eq. (1) read  $\mathcal{R}_{jj}^{\pm} = (\mathcal{R}_{Sj}^{\pm} + \mathcal{R}_{Aj}^{\pm})/2$  and  $\mathcal{R}_{ij}^{\pm} \approx (\mathcal{R}_{Si}^{\pm} + \mathcal{R}_{Sj}^{\pm} - \mathcal{R}_{Ai}^{\pm} - \mathcal{R}_{Aj}^{\pm})/4$ . Here,  $\mathcal{R}_{\lambda j}^{\pm}$  are the heating and cooling rates arising from the sidebands of the symmetric ( $\lambda = S$ ) and antisymmetric ( $\lambda = A$ ) spin states, and are obtained from Eq. (2) with the substitution  $\gamma \rightarrow \gamma_{\lambda}$ ,  $\Delta \rightarrow \Delta_{\lambda} \equiv \omega_L - \omega_{\lambda}$  and a modified diffusion rate [32]. Due to the dipole splitting  $J_{12}$ , the laser drive cannot be resonant with both collective cooling sidebands [see Fig. 1(b)]. Because of its reduced linewidth, we consider the drive on resonance with the cooling sideband of the antisymmetric state,  $\Delta = -\sqrt{\nu_1^2 + (\gamma_A/2)^2} - J_{12}$ . In Fig. 2(a), we plot the final average steady state population as a function of  $\Omega$  and  $\delta\nu \equiv |\nu_1 - \nu_2|$ . We identify three different cooling regimes.

The first regime, which we call “single-mode cooling” regime, corresponds to  $\delta\nu \ll \max\{V_{12}, \mathcal{R}_{12}^{\pm}\} \approx 2\eta^2\Omega^2/\gamma_A$ , such that the motional degrees of freedom of both atoms are resonantly coupled. We can then approximate  $\nu_1 \simeq \nu_2 = \nu$ , which results in a symmetrical configuration where the center-of-mass and relative motion are decoupled. The problem thus reduces to two instances of sideband cooling of a single atom, whereby the center-of-mass and relative motion are respectively cooled by the symmetric and antisymmetric spin states

at the rates  $\mathcal{R}_{S1}$  and  $\mathcal{R}_{A1}$  [35] [Fig. 1(c)]. In the resolved sideband regime  $\nu \gg \gamma_S$  and neglecting the recoil term, the optimal steady state phonon number of each mode is thus  $\bar{n}_A \approx (\gamma_A/4\nu)^2$  and  $\bar{n}_S \approx (\gamma_S^2 + 16J_{12}^2)/(4\nu)^2$ . Notably,  $\bar{n}_A \ll \bar{n}_{ind}$  due to the reduced linewidth of the anti-symmetric mode. The average phonon number per atom  $\bar{n} \equiv (\bar{n}_A + \bar{n}_S)/2$ , however, can never be lower than that of two non-interacting atoms.

The second or “array cooling” regime allows for enhanced cooling of both atoms, and is reached for

$$\frac{2\eta^2\Omega^2}{\gamma_A} \ll \delta\nu \ll \frac{\gamma_A}{2}. \quad (3)$$

The right condition in Eq. (3) ensures that the antisymmetric cooling sideband is simultaneously on resonance for both atoms. The left condition guarantees that the couplings  $V_{ij}$  and  $\mathcal{R}_{ij}^{\pm}$  between different atoms  $i \neq j$  in Eq. (1) can be neglected under the rotating wave approximation. In this regime, the exchange of motional quanta between different atoms is suppressed and the atoms are cooled independently at a rate  $\mathcal{R}_{11}^- \approx \mathcal{R}_{22}^- \approx \mathcal{R}_{A1}^-/2$ . Crucially, the cooling of both atoms is predominantly dictated by the properties of the subradiant antisymmetric spin mode [Fig. 1(d)]. At small interparticle distances, this leads to a lower average temperature as compared to the non-interacting case across a wide range of average trap frequencies  $\bar{\nu} = (\nu_1 + \nu_2)/2$  [Fig. 2(a) and (b)]. To quantify the enhancement in the cooling performance, we compute  $\bar{n}/\bar{n}_{ind}$  and unveil three different scenarios depending on the magnitude of  $\bar{\nu}$ .

(i) For  $\bar{\nu} \gg \gamma_S \simeq \gamma_0$ , the sidebands are resolved both in the case of interacting and non-interacting atoms, and the normalized phonon number is given as

$$\frac{\bar{n}}{\bar{n}_{\text{ind}}^{(\text{sc})}} \approx \frac{2\gamma_A}{\gamma_0}. \quad (4)$$

(ii) For  $\gamma_A \ll \bar{\nu} \lesssim \gamma_0$ , only the sidebands associated to the antisymmetric subradiant spin state are resolved. In this case, the normalized phonon number reads

$$\frac{\bar{n}}{\bar{n}_{\text{ind}}^{(\text{dc})}} \approx \frac{5}{28} \frac{\gamma_A^2}{\bar{\nu}\gamma_0}. \quad (5)$$

Remarkably, ground-state cooling can be achieved in this scenario even when the sidebands of an individual atom are *not* resolved and thus  $\bar{n}_{\text{ind}}^{(\text{dc})} \gtrsim 1$ .

(iii) For  $\bar{\nu} \ll \gamma_A/2$ , neither the collective nor the independent sidebands are resolved, and the system cannot be ground-state cooled. However, the optimal phonon number is still lower than that of non-interacting atoms,

$$\frac{\bar{n}}{\bar{n}_{\text{ind}}^{(\text{dc})}} \approx \frac{5}{7} \frac{\gamma_A}{\gamma_0}. \quad (6)$$

As shown in Fig. 2(c), the predictions of Eqs. (4)-(6) are in good agreement with the results obtained from the effective master equation (1) (solid lines) and from the full model including the internal dynamics (diamond markers) for different spacings  $d$  and trap frequencies  $\bar{\nu}$ .

The third and final regime in Fig. 2(a) corresponds to the condition  $\gamma_A \ll \delta\nu$ . In this case, the antisymmetric cooling sideband cannot be simultaneously on resonance with both atoms, and enhanced cooling is only possible for one atom, such that  $\bar{n}_1 < \bar{n}_{\text{ind}}$  but  $\bar{n}_2 > \bar{n}_{\text{ind}}$  [36, 37]. We refer to it as the “single atom cooling” regime.

Let us now consider the effect of dipole interactions on the cooling rate  $\Gamma$ . In the array cooling regime and when the subradiant sidebands are resolved, we obtain from Eq. (1) that  $\Gamma \simeq (\eta\Omega)^2/\gamma_A$ . That is, larger drive strengths  $\Omega$  lead to larger  $\Gamma$ , but eventually result in higher steady state phonon numbers because either Eq. (3) or the weak coupling condition  $\eta\Omega \ll \gamma_A$  is violated. Numerically solving the full system of coupled spin and motion, we compute the critical cooling rate  $\Gamma_c$ , defined as the one obtained at the driving strength  $\Omega_c$  that leads to a steady state phonon number 10% larger than the optimal one predicted by Eq. (1) [see white line in Fig. 2(a)]. We plot these results in Fig. 2(d) for  $\bar{\nu} = 20\gamma_0$ . At small  $\delta\nu \ll \gamma_A/2$ ,  $\Gamma_c \propto \delta\nu$  is limited by Eq. (3) and is smaller than in the case of non-interacting atoms. Increasing  $\delta\nu$ , the weak coupling condition is eventually violated, and at the critical driving strength  $\Omega_c$ , the rate  $\Gamma_c$  saturates to values similar to that of non-interacting atoms. For  $\bar{\nu} = 0.25\gamma_0$  [Fig. 2(e)], the motional sidebands are only resolved via the collective subradiant mode [scenario (ii) above] and the cooling rate can exceed that of

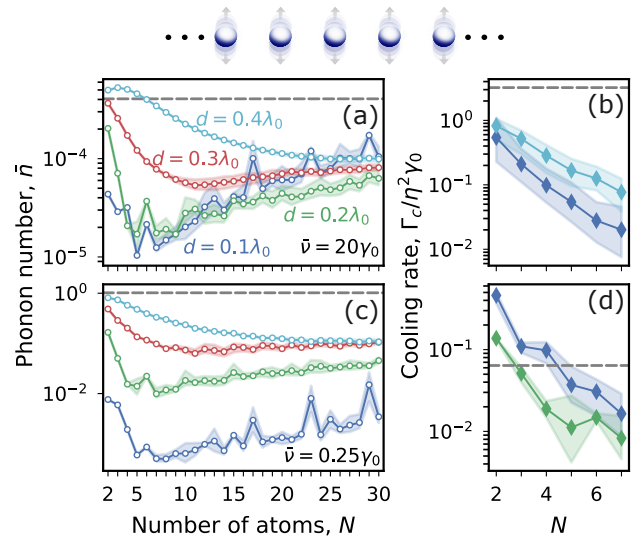


Figure 3. Sideband cooling of a chain of  $N$  interacting atoms. (a) Steady state phonon number per atom  $\bar{n}$  and (b) critical cooling rate  $\Gamma_c/\eta^2\gamma_0$  as a function of  $N$  for various spacings  $d$  and normally distributed trap frequencies with mean  $\bar{\nu} = 20\gamma_0$  and standard deviation  $\sigma = 10^{-3}\gamma_0$ . The drive frequency is chosen on resonance with the subradiant spin mode resulting in the smallest  $\bar{n}$ . We omit the cooling rates for  $d = 0.2\lambda_0$  and  $d = 0.3\lambda_0$ , which exhibit similar trends and values. (c-d) Analogous for  $\bar{\nu} = 0.25\gamma_0$ . In all panels, we plot the median (markers), as well as the 25-th to 75-th percentile region (shaded area) obtained by averaging over 300 realizations. Diamond markers and empty circles correspond respectively to the solution of the full system of equations and to the solution of Eq. (1). The grey dashed lines correspond to the case of non-interacting atoms  $d \gg \lambda_0$ .

non-interacting atoms. In this scenario, the subradiant collective spin mode allows to cool the atoms to much lower temperatures and at much faster time scales.

### $N$ interacting atoms

The fundamental concepts introduced above can be generalized to larger systems. In the following, we focus on ordered chains of  $N$  atoms, although similar conclusions hold for other arrangements (see SM [32]). The rates  $\mathcal{R}_{ij}^{\pm}$  in Eq. (1) contain contributions from all the  $N$  collective spin states of the system. In particular, each state contributes with a term of the same form as Eq. (2) where the linewidth is replaced by the collective decay rate and the detuning is centered at the collective resonance. However, the emergence of energy shifts between the different collective spin states implies that only one spin state can significantly contribute to the cooling dynamics. For finite arrays, cooling is attained if (i) the driving field is on resonance with the cooling sideband of a subradiant state with decay rate  $\gamma_d$ , (ii) this state

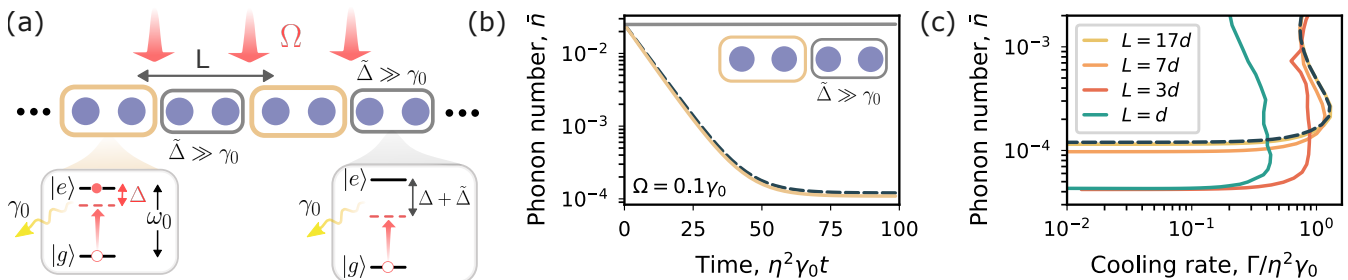


Figure 4. Protocol for sequential cooling. (a) Distant blocks of a few atoms (orange boxes) are cooled simultaneously, while the spin transition of the remaining atoms (grey boxes) is detuned by an additional shift  $\tilde{\Delta} \gg \gamma_0$ . Blocks of resonant atoms that are sufficiently far apart ( $L \gtrsim \lambda_0$ ) are cooled independently. (b) Cooling of a four-atom chain with spacing  $d = 0.15\lambda_0$ , where the last two atoms are far detuned by  $\tilde{\Delta} = -40\gamma_0$  (i. e.,  $L = d$ ). Light on resonance with the cooling sideband associated to the first two atoms (orange trace) leads to cooling with the same properties as for a chain of two atoms (black dashed line). The phonon number of the detuned atoms remains constant (grey line). (c) Steady state phonon number  $\bar{n}$  versus cooling rate  $\Gamma$  for four atoms located along the  $x$ -axis at positions  $x_1 = 0$ ,  $x_2 = d$ ,  $x_3 = L + d$  and  $x_4 = L + 2d$  for  $d = 0.15\lambda_0$ . The different pairs of  $\bar{n}$  and  $\Gamma$  are obtained by scanning the drive strength  $\Omega$ . The cooling properties of a two-atom chain (dashed lines) is recovered at large  $L$ . We consider  $\eta = 0.02$  and  $\nu_j = \bar{\nu} + \delta\nu(j - 3)$  with  $\bar{\nu} = 20\gamma_0$  and  $\delta\nu = 10^{-3}\gamma_0$ .

is delocalized (because only atoms where the collective state has a non-zero amplitude are cooled), and (iii)  $\forall i, j$ ,  $|\nu_i - \nu_j|$  satisfies Eq. (3) with  $\gamma_A$  substituted by  $\gamma_d$ . Notably, enhanced cooling does not require precise control of the trap frequency difference. Assuming  $\nu_j$  to be normally distributed with mean  $\bar{\nu}$  and standard deviation  $\sigma = 10^{-3}\gamma_0$  and setting the drive frequency on resonance with the cooling sideband of the optimal subradiant spin mode (i. e., the one leading to the smallest steady state phonon number) [38], we obtain enhanced cooling for subwavelength arrays of up to  $N = 30$  atoms both for the resolved ( $\bar{\nu} = 20\gamma_0$ ) and unresolved ( $\bar{\nu} = 0.25\gamma_0$ ) regimes, as shown in Fig. 3(a) and (c) respectively. Similar to the two-atom case, the enhancement is more pronounced for  $\bar{\nu} = 0.25\gamma_0$ , when the single-atom sidebands are not resolved but the collective subradiant sidebands are. As  $N$  grows, the steady state phonon number increases. This happens because the cooling region is reduced as  $\gamma_d$  decreases for larger arrays, and it becomes harder to satisfy Eq. (3) for all trap frequency pairs  $|\nu_i - \nu_j|$  simultaneously [39]. Note also that, for certain polarizations, a heating and a cooling sideband can become resonant when  $\bar{\nu}$  is of the order of the dipole energy splitting between collective modes, thereby leading to an overall heating of the system [32].

In Fig. 3(b,d), we show the optimal cooling rate  $\Gamma_c$  defined as for the two-atom case.  $\Gamma_c$  decreases with atom number independently of  $\bar{\nu}$ . We attribute this behavior to the narrowing of  $\gamma_d \gtrsim \eta^2 \gamma_0$ , and to the fact that only one delocalized subradiant spin mode can significantly contribute to cooling due to the collective energy shifts.

Cooling rates can be increased using different methods, such as applying multiple driving fields, each on resonance with a different subradiant cooling sideband [32]. Alternatively, faster cooling of large arrays can also be

attained by sequentially cooling groups of atoms, as sketched in Fig. 4(a). For that, we define a group of target atoms to be cooled (denoted by the orange boxes) and detune the spin transition of the remaining atoms (grey boxes) by an additional large amount  $|\tilde{\Delta}| \gg \gamma_0$ . Cooling at fast rates requires the target atoms to be arranged into blocks of a few adjacent atoms with large separations  $L \gtrsim \lambda_0$  between blocks [Fig. 4(a)]. The protocol relies on two key features. The first feature is that the detuned atoms do not affect the radiative properties of the target atoms and consequently do not modify their cooling process. This is exemplified in Fig. 4(b), where the two resonant atoms of a four-atom chain (orange trace) are cooled to the same phonon number and at the same rate as an array of just two atoms (black dashed trace). Importantly, the cooling and heating rates associated to the detuned atoms are much smaller than the cooling rates  $\Gamma$  associated to the target atoms, such that the phonon number of the detuned atoms remains constant over the timescales  $\sim \Gamma^{-1}$  considered. The second feature is that sufficiently separated blocks of atoms exhibit the same radiative properties as a single block. This is exemplified in Fig. 4(c), where we consider two blocks of two atoms such that the first and third atoms are at a distance  $L$ . Scanning the drive strength  $\Omega$ , we obtain the cooling rate  $\Gamma$  as a function of steady state phonon number  $\bar{n}$  for various  $L$ . As  $L$  increases, the maximum cooling rate tends to that of a two-atom chain (black dashed trace) and becomes significantly larger than that of four adjacent atoms (green trace for  $L = d$ ). Of course, the corresponding  $\bar{n}$  also increases to that of a two-atom chain. Combining both features, it becomes possible to cool multiple blocks of atoms to the same phonon number and at the same rate of a single block. Repeating the procedure for the atoms that were initially detuned, one

can sequentially cool large atomic arrays in a few steps, and thereby reduce the required time significantly.

### Conclusion and outlook

We have identified the general condition for ground-state sideband-cooling of dipole interacting atoms to temperatures lower than attainable in the absence of interactions. This condition is independent of the average value of the trap frequencies, and relies on the combinations of two factors: the emergence of narrowed collective linewidths in atomic arrays, and the suppression of motional interactions by trapping atoms with different trap frequencies. Our results are directly applicable to arrays of alkaline-earth and rare-earth atoms, which exhibit long-wavelength transitions [40, 41] and can be trapped at subwavelength separations using metasurface holographic optical traps [42], optical tweezer arrays [43] or optical lattices [8, 44, 45]. Our work could be further generalized to non-magic trapping conditions, for which the trapping potentials of the ground- and excited state differ [8, 10, 46]. Additionally, the single-atom cooling regime suggests the possibility to cool a large dilute array of atoms via the subradiant modes of a denser atomic lattice, which in turn heats up [27, 47]. More broadly, our work demonstrates that dipolar interactions can improve control over the motional state of atoms in arrays. Beside cooling, these methods could be used to generate squeezed states of motion or even correlated states of internal and external dynamics with a modified collective optical response [15]. Finally, the concepts explored here extend beyond trapped neutral atoms. They could be used to cool cantilevers coupled to a dense ensemble of interacting emitters [48], and suggest a method to cool multiple levitated nanoparticles [49, 50] in a cavity [51].

### Acknowledgments

O.R.B. acknowledges support from Fundaci3n Mauricio y Carlota Botton and from Fundaci3n Bancaria “la Caixa” (LCF/BQ/AA18/11680093). R.H. acknowledges funding by the Austrian Science Fund (FWF) 10.55776/W1259. SFY thanks the NSF through PHY-2207972, the CUA PFC PHY-2317134, and the Q-SEnSE QLCI OMA-2016244. A. A.-G. acknowledges support from the AFOSR through their Young Investigator Prize (No. 21RT0751), from the NSF through their CAREER Award (No. 2047380), and from the David and Lucile Packard Foundation. C.C.R. acknowledges support from the European Union’s Horizon Europe program under the Marie Sklodowska Curie Action LIME (Grant No. 101105916).

\* orubies@mit.edu

† cr3327@columbia.edu

- [1] D. E. Chang, J. S. Douglas, A. Gonz3lez-Tudela, C.-L. Hung, and H. J. Kimble, Colloquium: Quantum matter built from nanoscopic lattices of atoms and photons, *Rev. Mod. Phys.* **90**, 031002 (2018).
- [2] M. Reitz, C. Sommer, and C. Genes, Cooperative quantum phenomena in light-matter platforms, *PRX Quantum* **3**, 010201 (2022).
- [3] J. Ruostekoski, Cooperative quantum-optical planar arrays of atoms, *Phys. Rev. A* **108**, 030101 (2023).
- [4] R. J. Bettles, S. A. Gardiner, and C. S. Adams, Enhanced optical cross section via collective coupling of atomic dipoles in a 2d array, *Phys. Rev. Lett.* **116**, 103602 (2016).
- [5] E. Shahmoon, D. S. Wild, M. D. Lukin, and S. F. Yelin, Cooperative resonances in light scattering from two-dimensional atomic arrays, *Phys. Rev. Lett.* **118**, 113601 (2017).
- [6] A. Asenjo-Garcia, M. Moreno-Cardoner, A. Albrecht, H. J. Kimble, and D. E. Chang, Exponential improvement in photon storage fidelities using subradiance and “selective radiance” in atomic arrays, *Phys. Rev. X* **7**, 031024 (2017).
- [7] O. Rubies-Bigorda, V. Walther, T. L. Patti, and S. F. Yelin, Photon control and coherent interactions via lattice dark states in atomic arrays, *Phys. Rev. Res.* **4**, 013110 (2022).
- [8] J. Rui, D. Wei, A. Rubio-Abadal, S. Hollerith, J. Zeiher, D. M. Stamper-Kurn, C. Gross, and I. Bloch, A subradiant optical mirror formed by a single structured atomic layer, *Nature* **583**, 369 (2020).
- [9] A. Glicenstein, G. Ferioli, N. Šibalić, L. Brossard, I. Ferrier-Barbut, and A. Browaeys, Collective shift in resonant light scattering by a one-dimensional atomic chain, *Phys. Rev. Lett.* **124**, 253602 (2020).
- [10] K. Srakaew, P. Weckesser, S. Hollerith, D. Wei, D. Adler, I. Bloch, and J. Zeiher, A subwavelength atomic array switched by a single rydberg atom, *Nature Physics* **19**, 714 (2023).
- [11] P. R. Berman, Resonant interaction between identical atoms including recoil, *Phys. Rev. A* **55**, 4466 (1997).
- [12] R. N. Palmer and A. Beige, Enhancing laser sideband cooling in one-dimensional optical lattices via the dipole interaction, *Phys. Rev. A* **81**, 053411 (2010).
- [13] D. E. Chang, J. I. Cirac, and H. J. Kimble, Self-organization of atoms along a nanophotonic waveguide, *Phys. Rev. Lett.* **110**, 113606 (2013).
- [14] F. m. c. Damanet, D. Braun, and J. Martin, Master equation for collective spontaneous emission with quantized atomic motion, *Phys. Rev. A* **93**, 022124 (2016).
- [15] P.-O. Guimond, A. Grankin, D. V. Vasilyev, B. Vermersch, and P. Zoller, Subradiant bell states in distant atomic arrays, *Phys. Rev. Lett.* **122**, 093601 (2019).
- [16] A. T. Gisbert, N. Piovella, and R. Bachelard, Stochastic heating and self-induced cooling in optically bound pairs of atoms, *Phys. Rev. A* **99**, 013619 (2019).
- [17] A. T. Gisbert, N. Piovella, and R. Bachelard, Cooperative cooling in a one-dimensional chain of optically bound cold atoms, *Phys. Rev. A* **102**, 013312 (2020).

- [18] F. Robicheaux and S. Huang, Atom recoil during coherent light scattering from many atoms, *Phys. Rev. A* **99**, 013410 (2019).
- [19] E. Shahmoon, M. D. Lukin, and S. F. Yelin, Chapter one - collective motion of an atom array under laser illumination (Academic Press, 2019) pp. 1–38.
- [20] E. Shahmoon, M. D. Lukin, and S. F. Yelin, Quantum optomechanics of a two-dimensional atomic array, *Phys. Rev. A* **101**, 063833 (2020).
- [21] D. A. Suresh and F. Robicheaux, Photon-induced atom recoil in collectively interacting planar arrays, *Phys. Rev. A* **103**, 043722 (2021).
- [22] D. Hümmer, P. Schneeweiss, A. Rauschenbeutel, and O. Romero-Isart, Heating in nanophotonic traps for cold atoms, *Phys. Rev. X* **9**, 041034 (2019).
- [23] C. Monroe, D. M. Meekhof, B. E. King, S. R. Jefferts, W. M. Itano, D. J. Wineland, and P. Gould, Resolved-sideband raman cooling of a bound atom to the 3d zero-point energy, *Phys. Rev. Lett.* **75**, 4011 (1995).
- [24] D. J. Wineland, C. Monroe, W. M. Itano, D. Leibfried, B. E. King, and D. M. Meekhof, Experimental issues in coherent quantum-state manipulation of trapped atomic ions, *Journal of research of the National Institute of Standards and Technology* **103**, 259 (1998).
- [25] J. Eschner, G. Morigi, F. Schmidt-Kaler, and R. Blatt, Laser cooling of trapped ions, *JOSA B* **20**, 1003 (2003).
- [26] C. C. Rusconi, T. Shi, and J. I. Cirac, Exploiting the photonic nonlinearity of free-space subwavelength arrays of atoms, *Phys. Rev. A* **104**, 033718 (2021).
- [27] O. Rubies-Bigorda and et. al., Collective cooling of an ensemble of emitters, In preparation.
- [28] J. I. Cirac, R. Blatt, P. Zoller, and W. D. Phillips, Laser cooling of trapped ions in a standing wave, *Physical Review A* **46**, 2668 (1992).
- [29] C. Cohen-Tannoudji, Atomic motion in laser light, *Fundamental systems in quantum optics* **53**, 1 (1990).
- [30] C. Gardiner and P. Zoller, *The quantum world of ultracold atoms and light book II: the physics of quantum-optical devices*, Vol. 4 (World Scientific Publishing Company, 2015) pp. 228–240.
- [31] The steady state phonon number and cooling rates in the Doppler cooling regime are readily found by expanding  $\bar{n}_{\text{ind}}^{(dc)} = \mathcal{R}_{jj}^+ / (\mathcal{R}_{jj}^- - \mathcal{R}_{jj}^+)$  and  $\Gamma_{\text{ind}}^{(dc)} = \mathcal{R}_{jj}^- - \mathcal{R}_{jj}^+$  to leading order in  $\gamma_0/\nu$ .
- [32] See the Supplemental Material for: (i) the analytical derivations for the two-atom system; (ii) a detailed analysis of the role of the transition dipole moment, the direction of motion and the geometry; (iii) and a discussion on additional cooling strategies..
- [33] R. H. Lehmburg, Radiation from an  $n$ -atom system. ii. spontaneous emission from a pair of atoms, *Phys. Rev. A* **2**, 889 (1970).
- [34] A. Beige and G. C. Hegerfeldt, Cooperative effects in the light and dark periods of two dipole-interacting atoms, *Phys. Rev. A* **59**, 2385 (1999).
- [35] Note that  $\mathcal{R}_{\lambda 1} = \mathcal{R}_{\lambda 2}$  for  $\nu_1 = \nu_2$ .
- [36] C.-H. Wang, Y.-C. Wang, C.-C. Chen, C.-C. Wang, and H. H. Jen, Enhanced dark-state sideband cooling in trapped atoms via photon-mediated dipole-dipole interactions, *Phys. Rev. A* **107**, 023117 (2023).
- [37] C.-C. Chen, Y.-C. Wang, C.-C. Wang, and H. H. Jen, Chiral-coupling-assisted refrigeration in trapped ions, *Journal of Physics B: Atomic, Molecular and Optical Physics* **56**, 105502 (2023).
- [38] For a subradiant spin mode with collective linewidth  $\gamma_d$  and energy shift  $J_d$ , the drive is applied at the frequency  $\Delta = -\sqrt{\bar{\nu}^2 + (\gamma_d/2)^2} + J_d$ .
- [39] At large atom number  $N$ , the phonon number also increases due to the fact that multiple spin modes contribute to heating, while only one spin mode significantly contributes to cooling.
- [40] B. Olmos, D. Yu, Y. Singh, F. Schreck, K. Bongs, and I. Lesanovsky, Long-Range Interacting Many-Body Systems with Alkaline-Earth-Metal Atoms, *Physical Review Letters* **110**, 143602 (2013).
- [41] S. J. Masson, J. P. Covey, S. Will, and A. Asenjo-Garcia, Dicke superradiance in ordered arrays of multilevel atoms, *arXiv preprint arXiv:2304.00093* (2023).
- [42] X. Huang, W. Yuan, A. Holman, M. Kwon, S. J. Masson, R. Gutierrez-Jauregui, A. Asenjo-Garcia, S. Will, and N. Yu, Metasurface holographic optical traps for ultracold atoms, *Progress in Quantum Electronics* , 100470 (2023).
- [43] A. Cooper, J. P. Covey, I. S. Madjarov, S. G. Porsev, M. S. Safronova, and M. Endres, Alkaline-earth atoms in optical tweezers, *Physical Review X* **8**, 041055 (2018).
- [44] A. Derevianko and H. Katori, Colloquium: Physics of optical lattice clocks, *Rev. Mod. Phys.* **83**, 331 (2011).
- [45] S. Buob, J. Höschele, V. Makhlov, A. Rubio-Abadal, and L. Tarruell, A strontium quantum-gas microscope, *PRX Quantum* **5**, 020316 (2024).
- [46] T. D. Karanikolaou, R. J. Bettles, and D. E. Chang, Near-resonant light scattering by an atom in a state-dependent trap (2024), *arXiv:2401.06753 [quant-ph]*.
- [47] F. Shah, T. L. Patti, O. Rubies-Bigorda, and S. F. Yelin, Quantum computing with subwavelength atomic arrays, *Phys. Rev. A* **109**, 012613 (2024).
- [48] D. Zoepfl, M. L. Juan, N. Diaz-Naufal, C. M. F. Schneider, L. F. Deeg, A. Sharafiev, A. Metelmann, and G. Kirchmair, Kerr enhanced backaction cooling in magnetomechanics, *Phys. Rev. Lett.* **130**, 033601 (2023).
- [49] J. Piotrowski, D. Windey, J. Vijayan, C. Gonzalez-Ballester, A. de los Ríos Sommer, N. Meyer, R. Quidant, O. Romero-Isart, R. Reimann, and L. Novotny, Simultaneous ground-state cooling of two mechanical modes of a levitated nanoparticle, *Nature Physics* **19**, 1009 (2023).
- [50] J. Vijayan, J. Piotrowski, C. Gonzalez-Ballester, K. Weber, O. Romero-Isart, and L. Novotny, Cavity-mediated long-range interactions in levitated optomechanics, *Nature Physics* [10.1038/s41567-024-02405-3](https://doi.org/10.1038/s41567-024-02405-3) (2024).
- [51] O. S. Mishina, Cavity cooling of an atomic array, *New Journal of Physics* **16**, 033021 (2014).
- [52] I. Wilson-Rae, N. Nooshi, J. Dobrindt, T. J. Kippenberg, and W. Zwerger, Cavity-assisted backaction cooling of mechanical resonators, *New Journal of Physics* **10**, 095007 (2008).
- [53] C. Gonzalez-Ballester, Tutorial: projector approach to open quantum systems (2023), *arXiv:2305.19704 [quant-ph]*.
- [54] J. M. Torres, Closed-form solution of lindblad master equations without gain, *Phys. Rev. A* **89**, 052133 (2014).
- [55] S. Krämer, D. Plankensteiner, L. Ostermann, and H. Ritsch, Quantumoptics.jl: A julia framework for simulating open quantum systems, *Computer Physics Communications* **227**, 109 (2018).
- [56] D. Manzano, A short introduction to the lindblad master equation, *Aip Advances* **10** (2020).

## APPENDIX

### Formalism

In this section, we present the master equation for the full coupled dynamics of the internal and external degrees of freedom of atoms in a subwavelength atomic array in the Lamb-Dicke regime.

We consider an ensemble of  $N$  two-level atoms with transition frequency  $\omega_0 = ck_0 = 2\pi c/\lambda_0$  and lowering operators  $\hat{\sigma}_j \equiv |g_j\rangle\langle e_j|$ . The atoms are harmonically trapped at the sites  $\mathbf{R}_j$  of an ordered lattice with only one atom per lattice site, and driven by an external monochromatic laser at frequency  $\omega_L = \omega_0 + \Delta$  along  $\mathbf{k}_L$ . In the following we assume the system to be in the Lamb-Dicke regime, namely the following condition holds  $\forall j$

$$\eta_j \equiv (2n_{\text{th}} + 1)\sqrt{\frac{\nu_R}{\nu_j}} \ll 1, \quad (7)$$

where  $\nu_R \equiv \hbar k_0^2/2m$  is the atomic recoil frequency, and  $n_{\text{th}}$  is the thermal occupation number of the atomic center of mass motion in the local harmonic trap. Equation (7) generally holds when the atoms are confined by the harmonic trap in a region much smaller than the resonant wavelength  $\lambda_0$ . In this case the atomic fluctuations around the trapping site are small and can be treated perturbatively. We assume the atoms to move along one direction  $\mathbf{e}_\alpha$  ( $\alpha = x, y, z$ ). Tracing out the electromagnetic vacuum field under the Born-Markov approximation and keeping terms up to second order in the position fluctuations (that is to second order in  $\eta_j$ ), we derive the master equation describing the internal (spin) and external (motion) degrees of freedom in the Lamb-Dicke regime. It reads

$$\frac{d}{dt}\hat{\rho}_{\text{tot}} = -\frac{i}{\hbar}\left(\hat{H}_{\text{tot}}\hat{\rho}_{\text{tot}} - \hat{\rho}_{\text{tot}}\hat{H}_{\text{tot}}^\dagger\right) + \mathcal{D}_t(\hat{\rho}_{\text{tot}}). \quad (8)$$

Here, we defined the non-Hermitian Hamiltonian  $\hat{H}_{\text{tot}} \equiv \hat{H} + \hat{V}$ , where

$$\begin{aligned} \frac{\hat{H}}{\hbar} &\equiv \sum_j \left[ \nu_j \hat{b}_j^\dagger \hat{b}_j - \left( \Delta + i\frac{\gamma_0}{2} \right) \hat{\sigma}_j^\dagger \hat{\sigma}_j \right] + \sum_{i,j \neq i} G_{ij} \hat{\sigma}_i^\dagger \hat{\sigma}_j \\ &+ \sum_{i,j \neq i} \left[ G'_{ij} (\eta_i \hat{r}_i - \eta_j \hat{r}_j) + \frac{1}{2} G''_{ij} (\eta_i \hat{r}_i - \eta_j \hat{r}_j)^2 \right] \hat{\sigma}_i^\dagger \hat{\sigma}_j \end{aligned} \quad (9)$$

---


$$\mathcal{D}_t(\hat{\rho}_t) = \sum_{i,j} \gamma_{ij} \hat{\sigma}_j \hat{\rho}_t \hat{\sigma}_i^\dagger + \sum_{i,j \neq i} \gamma'_{ij} \left( \eta_i \hat{\sigma}_j \hat{\rho}_t \hat{\sigma}_i^\dagger \hat{r}_i - \eta_j \hat{r}_j \hat{\sigma}_j \hat{\rho}_t \hat{\sigma}_i^\dagger \right) + \sum_{i,j} \frac{\gamma''_{ij}}{2} \left( \eta_i^2 \hat{\sigma}_j \hat{\rho}_t \hat{\sigma}_i^\dagger \hat{r}_i \hat{r}_i - 2\eta_i \eta_j \hat{r}_j \hat{\sigma}_j \hat{\rho}_t \hat{\sigma}_i^\dagger \hat{r}_i + \eta_j^2 \hat{r}_j \hat{r}_j \hat{\sigma}_j \hat{\rho}_t \hat{\sigma}_i^\dagger \right), \quad (14)$$


---

where the second and third terms capture the collective

is the non-Hermitian Hamiltonian describing an array of dipole interacting atoms including the effects of atomic recoil along one direction, and

$$\hat{V} \equiv \sum_j \left[ \left( \Omega_j + \eta_j \Omega'_j \hat{r}_j + \frac{1}{2} \eta_j^2 \Omega''_j \hat{r}_j^2 \right) \hat{\sigma}_j^\dagger + \text{h.c.} \right], \quad (10)$$

is the driving Hamiltonian up to second order in the Lamb-Dicke expansion. Here,  $\hat{r}_j \equiv \hat{b}_j + \hat{b}_j^\dagger$ , where  $\hat{b}_n^\dagger$  ( $\hat{b}_n$ ) is the creation (annihilation) operator of a center of mass phonon for atom  $n$ . We also defined the position-dependent Rabi frequency  $\Omega_j \equiv \Omega \exp(i\mathbf{k}_L \cdot \mathbf{R}_j)$ , and  $\Omega'_j \equiv k_0^{-1} \partial_{R_{\alpha_j}} \Omega_j$  and  $\Omega''_j \equiv k_0^{-2} \partial_{R_{\alpha_j}}^2 \Omega_j$ . These latter two terms correspond to the first and second order Lamb-Dicke optomechanical forces exerted by the laser on the atoms. In Eq. (9), we defined the dipole coupling rate as

$$G_{ij} \equiv J_{ij} - i\frac{\gamma_{ij}}{2} = -\frac{3\pi\gamma_0}{k_0|\mathbf{d}|^2} \mathbf{d}^* \cdot \mathbf{G}(\mathbf{R}_i - \mathbf{R}_j, \omega_0) \cdot \mathbf{d}, \quad (11)$$

where  $\mathbf{d}$  represents the dipole moment of the atoms and

$$\begin{aligned} \mathbf{G}(\mathbf{R}, \omega) &= \frac{e^{ikR}}{4\pi k_0^2 R^3} \left[ (k_0^2 R^2 + ik_0 R - 1) \mathbb{1} \right. \\ &\left. + (-k_0^2 R^2 - 3ik_0 R + 3) \frac{\mathbf{R} \otimes \mathbf{R}}{R^2} \right] + \frac{\delta^{(3)}(\mathbf{R})}{3k_0^2} \mathbb{1}, \end{aligned} \quad (12)$$

with  $R = |\mathbf{R}|$  being the free space electromagnetic Green's tensor. In Eq. (11),  $J_{ij}$  and  $\gamma_{ij}$  represent respectively the coherent and dissipative dipole coupling rates between atom  $i$  and  $j$ . The spontaneous decay rate is equal for all atoms,  $\gamma_0 \equiv \gamma_{jj}$ . The dipole-mediated spin-motion coupling rate to first and second order in the Lamb-Dicke parameter are defined respectively as

$$\begin{aligned} G'_{ij} &\equiv J'_{ij} - i\frac{\gamma'_{ij}}{2} \equiv \frac{1}{k_0} \frac{\partial G(\mathbf{R})}{\partial R_\alpha} \Big|_{\mathbf{R}_i - \mathbf{R}_j}, \\ G''_{ij} &\equiv J''_{ij} - i\frac{\gamma''_{ij}}{2} \equiv \frac{1}{k_0^2} \frac{\partial^2 G(\mathbf{R})}{\partial R_\alpha^2} \Big|_{\mathbf{R}_i - \mathbf{R}_j}. \end{aligned} \quad (13)$$

The last term in Eq. (8) is the population recycling term describing the effects of quantum jumps on the total atomic state. It reads

photon emission accompanied by the collective recoil of



the atoms.

### Effective sideband cooling master equation

Let us now discuss the derivation of Eq. (1) in the main text. Here, we only sketch the derivation discussing the fundamental assumptions and approximations. The full derivation can be found in Ref. [27].

As for the case of a single atom or ion, an effective master equation for the atomic motion can be obtained under the assumption of weak spin-motion coupling, i.e., weaker than the decay rate of the internal dynamics [28, 52] (see also the recent tutorial [53]). As shown in Ref. [54], in the absence of spin-motion coupling, the timescale of the internal dynamics of the system can be determined by the zeroth-order Lamb-Dicke term of the non-Hermitian Hamiltonian in Eq. (9),

$$\frac{\hat{H}_S}{\hbar} = \sum_j \left( -\Delta - i\frac{\gamma_0}{2} \right) \hat{\sigma}_j^\dagger \hat{\sigma}_j + \sum_{i \neq j} \left( \bar{J}_{ij} - i\frac{\tilde{\gamma}_{ij}}{2} \right) \hat{\sigma}_i^\dagger \hat{\sigma}_j, \quad (15)$$

where we defined the couplings

$$\bar{J}_{ij} \equiv J_{ij} + \frac{\eta_i^2 + \eta_j^2}{2} J''_{ij}, \quad \tilde{\gamma}_{ij} \equiv \gamma_{ij} + \frac{\eta_i^2 + \eta_j^2}{2} \gamma''_{ij}. \quad (16)$$

Considering at most one spin excitation in the system (i.e., for weak or off-resonant drives), the spectrum of Eq. (15) reads  $\epsilon_\lambda = -\Delta + J_\lambda - i\gamma_\lambda/2$ , where the real and imaginary part describe the energy and decay rate of the system, and the single-excitation eigenstates read  $\hat{H}_S |\phi_\lambda\rangle = \kappa_\lambda |\phi_\lambda\rangle$ , with  $|\phi_\lambda\rangle = \sum_j \phi_{\lambda,j} \hat{\sigma}_j^\dagger |0\rangle$  for  $\lambda \in \{1, N\}$ . Note that in the limit of infinitely large atomic arrays, the system is translation invariant – to zero order in  $\eta$  – and the eigenstates are Bloch states with a well defined quasi momentum. Notably, the  $\eta^2$  correction to the dissipative interactions  $\tilde{\gamma}_{ij}$  sets a lower bound to the minimum achievable decay rate,  $\gamma_\lambda \gtrsim \eta^2 \gamma_0$ , and thereby prevents the system from exhibiting perfect dark states with zero decay rate [15, 26]. This is a crucial insight, that allows us to derive an effective master equation for subwavelength atomic arrays. This was not recognized before and thus previous treatment were limited to larger interatomic separations where the line narrowing effect is less prominent [12].

An effective master equation for the atomic motion can be derived when the interactions between the spin and motional degrees of freedom are smaller than the dissipative dynamics of the spins,  $\eta\Omega \ll \gamma_\lambda$  and  $\eta J'_{ij} \ll \gamma_\lambda$ , such that photon emission occurs at fast scales and the spin degrees of freedom can be adiabatically eliminated. Further, applying the rotating wave approximation and assuming that the atoms are only weakly driven such that their optical response can be linearized ( $\hat{\sigma}_j^\dagger \sim -1 \nabla_j$ ), which is valid when  $|\Omega_j| \ll (-\Delta + J_\lambda)^2 + \gamma_\lambda^2/4$  for all

states  $|\phi_\lambda\rangle$  directly driven by the field, we obtain the effective master equation for the density matrix  $\hat{\rho}_M$  of the motional degrees of freedom, given by Eq. (1) in the main text.

From Eq. (1), we derive the equations of motion for the expectation values of operators of the form  $\langle \hat{b}_i^\dagger \hat{b}_j \rangle$ ,

$$\begin{aligned} \frac{d}{dt} \langle \hat{b}_i^\dagger \hat{b}_j \rangle &= i(\nu_i + V_{ii} - \nu_j - V_{jj}) \langle \hat{b}_i^\dagger \hat{b}_j \rangle \\ &\quad - \left( \frac{\mathcal{R}_{ii}^- + \mathcal{R}_{jj}^-}{2} - \frac{\mathcal{R}_{ii}^+ + \mathcal{R}_{jj}^+}{2} \right) \langle \hat{b}_i^\dagger \hat{b}_j \rangle + \mathcal{R}_{ij}^+ \\ &\quad + \sum_{p \neq i} \left( iV_{pi} - \frac{\mathcal{R}_{pi}^-}{2} + \frac{\mathcal{R}_{ip}^+}{2} \right) \langle \hat{b}_p^\dagger \hat{b}_j \rangle \\ &\quad + \sum_{p \neq j} \left( -iV_{jp} - \frac{\mathcal{R}_{jp}^-}{2} + \frac{\mathcal{R}_{pj}^+}{2} \right) \langle \hat{b}_i^\dagger \hat{b}_p \rangle, \quad (17) \end{aligned}$$

Solving this coupled set of differential equations, we obtain the expectation value of the phonon number of each atom over time,  $n_j(t) = \langle \hat{b}_j^\dagger \hat{b}_j \rangle(t)$ . Setting the time derivatives to zero and solving the resulting linear set of equations, we obtain the expectation value of the phonon number of each atom in the steady state,  $\bar{n}_j = \lim_{t \rightarrow \infty} \langle \hat{b}_j^\dagger \hat{b}_j \rangle(t)$ , as well as the average steady state phonon number of the system,  $\bar{n} = \sum_j \bar{n}_j/N$ . These are the results that we plot in Fig. 2 and Fig. 3 in the main text.

Let us now describe the coupling terms appearing in Eq. (17). For simplicity, we consider from now on motion perpendicular to the axis defined by the positions of the atoms, such that  $J'_{ij} = \gamma'_{ij} = 0$ . The equations for the more general case are given in Ref. [27]. Then, the coherent coupling rates arising from the coherent evolution in Eq. (1) are

$$\begin{aligned} V_{jj} &= \eta_j^2 \sum_{i \neq j} \left( 2J''_{ji} \text{Re}\{s_j^{(0)} s_i^{*(0)}\} + \gamma''_{ji} \text{Im}\{s_j^{*(0)} s_i^{(0)}\} \right) \\ &\quad + 2\eta_j^2 \text{Re}\{\Omega_j'' s_j^{*(0)}\} + \Delta_{jj}^- + \Delta_{jj}^+, \quad (18a) \end{aligned}$$

$$V_{ij} = \Delta_{ij}^- + \Delta_{ji}^+ - 2\eta_i \eta_j J''_{ij} \text{Re}\{s_i^{(0)} s_j^{*(0)}\}, \quad (18b)$$

$$\Delta_{ij}^\pm = -\frac{1}{2} \eta_i \eta_j \Omega_j' \Omega_i^* \sum_\lambda \left( \frac{c_{\lambda,ij}}{\epsilon_\lambda \pm \nu_j} + \frac{c_{\lambda,ij}^*}{\epsilon_\lambda^* \pm \nu_i} \right), \quad (18c)$$

where  $\lambda$  labels the  $N$  eigenstates  $|\phi_\lambda\rangle$  of the non-Hermitian spin Hamiltonian, and  $c_{\lambda,ij} = \phi_{\lambda,i} \phi_{\lambda,j} / \sum_p \phi_{\lambda,p}^2$  describes the overlap of atoms  $i$  and  $j$  with the spin eigenstate  $|\phi_\lambda\rangle$ . Additionally, the complex numbers  $s_j^{(0)}$  describe the displacement of the atomic spins due to the weak drive to zeroth order in  $\eta_j$ , and are obtained from the coupled set of equations  $(-\Delta - i\gamma_0/2) s_i^{(0)} + \sum_{j \neq i} (J_{ij} - i\Gamma_{ij}/2) s_j^{(0)} = -\Omega_i$ . Finally, the second and third contributions to the master equation (1) in the main text correspond to a cooling and heating Lindbladian. They respectively describe

the correlated loss and gain of a phonon or motional quantum among multiple atoms at rates  $\mathcal{R}_{ij}^-$  and  $\mathcal{R}_{ij}^+$ , given by

$$\begin{aligned} \mathcal{R}_{ij}^\pm = & -i\eta_i\eta_j\Omega'_j\Omega_i^* \sum_\lambda \left( \frac{c_{\lambda,ij}}{\epsilon_\lambda \pm \nu_j} - \frac{c_{\lambda,ij}^*}{\epsilon_\lambda^* \pm \nu_i} \right) \\ & - \eta_i\eta_j\gamma''_{ij} s_j^{(0)} s_i^{*(0)}. \end{aligned} \quad (19)$$

The first term represents the cooling or heating arising from the spin-motion coupling introduced by the first-order Lamb-Dicke expansion of the driving Hamiltonian. Since photon emission occurs through the collective states  $|\phi_\lambda\rangle$ , it leads to the correlated dissipation of motional quanta in Eq. (1). Finally, the second term describes the recoil or diffusive motion of the atoms under collective photon emission, and its strength is therefore proportional to the amplitude in the spin excited states.

### Numerical simulation of the cooling dynamics

The results presented in this work are obtained either by solving the adiabatically eliminated equations (17) for the atomic motion only, or by numerically solving the master equation (8) for the full model taking into account both the spin and motional degrees of freedom.

In order to numerically solve Eq. (8), we employ the computational framework QuantumOptics.jl [55], which allows for a straightforward implementation of the equations on a computer. Nevertheless, the dimension of the Hilbert space of spin and motional degrees of freedom increases exponentially with the number of atoms  $N$ , namely  $\dim(\mathcal{H}) = 2^N \times N_{\text{cutoff}}^N$  where  $N_{\text{cutoff}}$  is the maximal number of motional excitations per atom. For two atoms, we solve the equations for  $N_{\text{cutoff}} = 2$ . For larger systems, this is no longer possible, and the numerical solution of Eq. (8) is only possible under the following assumptions. First, we consider that at most one atomic spin can be excited at a time, a valid approximation in the weak driving regime and for far off-resonant laser drives. Similarly, we also assume that the atoms share at most one phonon or motional quantum. Of course, this approximation is only valid when the subradiant spin state used for cooling is resolved and the steady state phonon number is significantly below one. Under these approximations, the dimension of the Hilbert space is reduced to  $\dim(\mathcal{H}) = (N+1)^2$ . Consequently, the total density matrix  $\hat{\rho}_{\text{tot}}$  in Eq. (8) has dimension  $(N+1)^2 \times (N+1)^2$  and its time evolution can be simulated up to 7 atoms. For that, we convert  $\hat{\rho}_{\text{tot}}$  into a vector  $\vec{\rho}_{\text{tot}}$  defined on a Fock-Liouville space [56]. Then, Eq. (8) can be recast as  $d\vec{\rho}_{\text{tot}}/dt = \mathcal{L}\vec{\rho}_{\text{tot}}$ , where  $\mathcal{L}$  is the Liouville superoperator describing both the effect of the Hamiltonian and the population recycling term. The state of the system over time is finally obtained via matrix exponentiation as  $\vec{\rho}_{\text{tot}}(t) = \exp(\mathcal{L}t)\vec{\rho}_{\text{tot}}(0)$ , where  $\vec{\rho}_{\text{tot}}(0)$

describes the initial density matrix describing both the spin and motional degrees of freedom. Finally, the cooling rate is extracted by fitting an exponential decaying phonon number over time.

# Collectively enhanced ground-state cooling in subwavelength atomic arrays

## Supplemental Material

Oriol Rubies-Bigorda<sup>1,2</sup>, Raphael Holzinger<sup>3</sup>, Ana Asenjo-Garcia<sup>4</sup>, Oriol Romero-Isart<sup>3,5</sup>, Helmut Ritsch<sup>3</sup>, Stefan Ostermann<sup>2</sup>, Carlos Gonzalez-Ballester<sup>6</sup>, Susanne Yelin<sup>2</sup>, and Cosimo C. Rusconi<sup>4</sup>.

<sup>1</sup>*Physics Department, Massachusetts Institute of Technology, Cambridge, Massachusetts 02139, USA.*

<sup>2</sup>*Department of Physics, Harvard University, Cambridge, Massachusetts 02138, USA.*

<sup>3</sup>*Institute for Theoretical Physics, University of Innsbruck, A-6020 Innsbruck, Austria.*

<sup>4</sup>*Department of Physics, Columbia University, New York, New York 10027, USA.*

<sup>5</sup>*Institute for Quantum Optics and Quantum Information of the Austrian Academy of Sciences, A-6020 Innsbruck, Austria.*

<sup>6</sup>*Institute for Theoretical Physics, Vienna University of Technology (TU Wien), 1040 Vienna, Austria*

### I. SIDEBAND COOLING OF TWO ATOMS

We consider now the case of two atoms trapped at a distance  $d$  on the  $x$ -axis and moving only along the  $z$ -direction as illustrated in Fig. 1(a). They are driven by a plane wave classical driving field propagating along  $\mathbf{z}$ , such that  $\Omega_j = \Omega$ ,  $\Omega'_j = i\Omega$  and  $\Omega''_j = -\Omega$  for  $j \in \{1, 2\}$ . It is instructive to explicitly write down the driving Hamiltonian for two atoms up to first order in the Lamb-Dicke regime,  $\hat{V} \equiv \hat{V}_0 + \hat{V}_1 + \mathcal{O}(\eta_j^2)$ . Considering up to one spin excitation in the system (i. e., in the low-excitation limit), it reads

$$\begin{aligned} \frac{\hat{V}_0}{\hbar} &\equiv \Omega\sqrt{2} \left( |S\rangle \langle gg| + \text{h.c.} \right), \\ \frac{\hat{V}_1}{\hbar} &\equiv \frac{i\Omega}{\sqrt{2}} \left[ |S\rangle \langle gg| (\eta_1 \hat{z}_1 + \eta_2 \hat{z}_2) + |A\rangle \langle gg| (\eta_1 \hat{z}_1 - \eta_2 \hat{z}_2) - \text{h.c.} \right]. \end{aligned} \quad (\text{S1})$$

Here we introduced the symmetric  $|S\rangle = (\hat{\sigma}_1^\dagger/\sqrt{2} + \hat{\sigma}_2^\dagger/\sqrt{2})|gg\rangle$  and the antisymmetric  $|A\rangle = (\hat{\sigma}_1^\dagger/\sqrt{2} - \hat{\sigma}_2^\dagger/\sqrt{2})|gg\rangle$  spin states. They are eigenstates of Eq. (15) with eigenvalues  $\epsilon_S \equiv \omega_0 + J_{12} - i\gamma_S/2$  and  $\epsilon_A \equiv \omega_0 - J_{12} - i\gamma_A/2$ , where we defined  $\gamma_S = \gamma_0 + \gamma_{12}$  and  $\gamma_A = \gamma_0 - \gamma_{12}$ . From Eq. (S1), we see that the first order Lamb-Dicke correction  $\hat{V}_1$  drives both symmetric and antisymmetric sidebands even when  $\hat{V}_0$  only excites the symmetric transition.

Noting that the displacement of the atomic spins is  $s_1^{(0)} = s_2^{(0)} = -\Omega/((J_{12} - \Delta) - i(\gamma_0 + \gamma_{12})/2)$ , we obtain the effective coupling rates for the coherent and dissipative evolution of the coupled motional degrees of freedom of both atoms in Eqs. (18a-19). In particular, the dissipative rates  $\mathcal{R}_{ij}^\pm$  are determined by the collective symmetric and anti-symmetric resonances,

$$\mathcal{R}_{Aj}^\pm \equiv \frac{\eta_j^2 \Omega^2 \gamma_A}{(-\Delta - J_{12} \pm \nu_j)^2 + (\gamma_A/2)^2} - \frac{\eta_j^2 \Omega^2 \gamma_A''}{(-\Delta + J_{12})^2 + (\gamma_S/2)^2}, \quad (\text{S2a})$$

$$\mathcal{R}_{Sj}^\pm \equiv \frac{\eta_j^2 \Omega^2 \gamma_S}{(-\Delta + J_{12} \pm \nu_j)^2 + (\gamma_S/2)^2} - \frac{\eta_j^2 \Omega^2 \gamma_S''}{(-\Delta + J_{12})^2 + (\gamma_S/2)^2}. \quad (\text{S2b})$$

The first term of the right hand side of Eq. (S2a) represents the cooling (−) and heating (+) sidebands of the antisymmetric collective mode  $|A\rangle$ , as illustrated in Fig. 1(b) in the main text. They are Lorentzians of width  $\gamma_A$  respectively centered at  $\Delta = -\nu_j - J_{12}$  and  $\Delta = \nu_j - J_{12}$ , with  $j \in \{1, 2\}$ . Notably, the center of the Lorentzians are shifted for both atoms by an amount equal to their trap frequency difference. Similarly, Eq. (S2b) represents the cooling (−) and heating (+) sidebands of the symmetric collective mode  $|S\rangle$ , respectively centered at  $\Delta = -\nu_j + J_{12}$  and  $\Delta = \nu_j + J_{12}$ . The second term in Eqs. (S2a) and (S2b) represents recoil heating due to scattering from the collective spin transition. Here,  $\gamma_S'' = \gamma_0'' + \gamma_{12}'' < 0$  and  $\gamma_A'' = \gamma_0'' - \gamma_{12}'' < 0$ , where we have defined  $\gamma_0'' \equiv \gamma_{jj}''$  equal for all atoms. Again, the contribution from the recoil or diffusive motion enters through a Lorentzian of width  $\gamma_S$  centered at  $\Delta = J_{12}$ . Note this Lorentzian is centered at the symmetric resonance both for  $\mathcal{R}_{Aj}^\pm$  and  $\mathcal{R}_{Sj}^\pm$  because  $\hat{V}_0$  only drives the symmetric transition,  $|gg\rangle \leftrightarrow |S\rangle$ . In terms of these quantities, the diagonal rates in Eq. (19) take the form

$$\mathcal{R}_{jj}^\pm = \frac{1}{2} \left( \mathcal{R}_{Aj}^\pm + \mathcal{R}_{Sj}^\pm \right), \quad (\text{S3})$$

while the off-diagonal terms can be approximated as  $\mathcal{R}_{ij}^\pm \approx (\mathcal{R}_{Si}^\pm + \mathcal{R}_{Sj}^\pm - \mathcal{R}_{Ai}^\pm - \mathcal{R}_{Aj}^\pm)/4$ .

Since the steady state phonon number for a single atom scales with its decay rate  $\gamma_0$ , cooling to lower temperatures in the case of multiple atoms requires the driving field to be on resonance with the cooling sideband associated to

the antisymmetric or subradiant spin state. For a given value of  $\nu/\gamma_0$ , cooling via the antisymmetric spin mode is maximized when  $\Delta = -\sqrt{\nu_1^2 + (\gamma_A/2)^2} - J_{12}$ . When the cooling and heating sidebands of the antisymmetric transition are resolved ( $\nu \gg \gamma_A$ ), this condition reduces to  $\Delta = -\nu_1 - J_{12}$ . However, due to the presence of dissipative  $\mathcal{R}_{ij}^\pm$  and coherent  $V_{ij}$  couplings between the motional degrees of freedom of different atoms, the lowest achievable steady state phonon numbers  $\bar{n}_j$  are *a priori* unclear. As we discuss in the following subsections,  $\bar{n}_j$  strongly depends on the trap frequency difference  $\delta\nu = |\nu_2 - \nu_1|$  between both atoms and the average trap frequency  $\bar{\nu} = (\nu_1 + \nu_2)/2$ .

### A. Single-mode cooling

Let us first consider the case of small trap frequency difference, defined as the values of  $\delta\nu$  for which

$$\delta\nu \ll \frac{2\eta_j^2\Omega^2}{\gamma_A}. \quad (\text{S4})$$

Together with the condition for adiabatic elimination of the spin degrees of freedom  $\eta\Omega \ll \gamma_A$ , Eq. (S4) also implies  $\delta\nu \ll \gamma_A/2$ . That is, the trap frequency difference between the atoms is much smaller than the widths of the Lorentzians of the cooling and heating sidebands, and we can simply write  $\mathcal{R}_{\lambda 2}^\pm \approx \mathcal{R}_{\lambda 1}^\pm \equiv \mathcal{R}_\lambda^\pm$  (for  $\lambda \in \{S, A\}$ ) and  $\eta \equiv \eta_1 \approx \eta_2$ . At the optimal detuning,  $\Delta = -\sqrt{\nu_1^2 + (\gamma_A/2)^2} - J_{12}$ , the dissipative coupling rate in Eq. (1) of the main text reads

$$\mathcal{R}_{12}^- \approx \frac{\mathcal{R}_S^- - \mathcal{R}_A^-}{2} \approx -2\frac{\eta^2\Omega^2}{\gamma_A} + 2\frac{\eta^2\Omega^2\gamma_S}{\gamma_S^2 + 16J_{12}^2} \approx -2\frac{\eta^2\Omega^2}{\gamma_A}, \quad (\text{S5})$$

and originates predominantly from the cooling sideband of the antisymmetric spin state. Note that the contribution from the symmetric spin mode [i. e., the second term in the second identity of Eq. (S5)] is suppressed at small atomic separations due to the wider superradiant resonance  $\gamma_S$  and the increasing energy shift  $2J_{12}$  between the cooling sidebands of both collective spin modes. From Eq. (S5), we interpret Eq. (S4) as the condition under which the dissipative coupling rates in Eq. (1) are resonant. In this case, the time-dependent phases  $e^{\pm i(\nu_1 - \nu_2)t}$  in Eq. (1) have no effect during the cooling process and can therefore be neglected. The effective master equation for the atomic motion becomes diagonal when considering the center-of-mass and relative motion of the atoms, defined through the operators  $\hat{b}_S = (\hat{b}_1 + \hat{b}_2)/\sqrt{2}$  and  $\hat{b}_A = (\hat{b}_1 - \hat{b}_2)/\sqrt{2}$ , and reads

$$\frac{d}{dt}\hat{\rho}_M = -i \left[ \sum_\lambda V_\lambda \hat{b}_\lambda^\dagger \hat{b}_\lambda, \hat{\rho}_M \right] + \sum_\lambda \mathcal{R}_\lambda^- \left( \hat{b}_\lambda \hat{\rho}_M \hat{b}_\lambda^\dagger - \frac{1}{2} \{ \hat{b}_\lambda^\dagger \hat{b}_\lambda, \hat{\rho}_M \} \right) + \sum_\lambda \mathcal{R}_\lambda^+ \left( \hat{b}_\lambda^\dagger \hat{\rho}_M \hat{b}_\lambda - \frac{1}{2} \{ \hat{b}_\lambda \hat{b}_\lambda^\dagger, \hat{\rho}_M \} \right), \quad (\text{S6})$$

with  $\lambda = \{A, S\}$ . In the resolved sideband regime  $\bar{\nu} \gg \gamma_0$  and for  $\bar{\nu} \gg J_{12}$ , the energy shifts of the center-of-mass and relative motional modes read

$$V_S \approx \frac{3\eta^2\Omega^2}{2\bar{\nu}} - \frac{2\eta^2\Omega^2 J_{12}}{4J_{12}^2 + (\gamma_S/2)^2} \quad V_A \approx \frac{3\eta^2\Omega^2}{2\bar{\nu}} + \frac{4\eta^2\Omega^2 J_{12}''}{\bar{\nu}^2}, \quad (\text{S7})$$

and are much smaller than  $\mathcal{R}_A^-$ . Notably, Eq. (S6) evidences that the center-of-mass and relative motion are decoupled and independently cooled according to the radiative properties of the symmetric and antisymmetric spin states, respectively. Then, the steady state phonon occupations  $\bar{n}_\lambda = \mathcal{R}_\lambda^+ / (\mathcal{R}_\lambda^- - \mathcal{R}_\lambda^+)$  in the resolved sideband regime are

$$\bar{n}_A \approx \frac{\gamma_A^2}{16\bar{\nu}^2} \left( 1 - 4\frac{\gamma_A''}{\gamma_A} \right), \quad (\text{S8})$$

$$\bar{n}_S \approx \frac{\gamma_S^2 + 16J_{12}^2}{16\bar{\nu}^2} \left( 1 - 4\frac{\gamma_S''}{\gamma_S} \right). \quad (\text{S9})$$

Compared to the steady state phonon number for non-interacting atoms,  $\bar{n}_{ind} \approx (\gamma_0^2 - 4\gamma_0\gamma_0'')/16\bar{\nu}^2$ ,  $\bar{n}_S$  and  $\bar{n}_A$  are modified by the decay rates of the collective spin states. At small distances between both atoms, the antisymmetric spin state  $|A\rangle$  becomes subradiant ( $\gamma_A < \gamma_0$  and  $|\gamma_A''| < |\gamma_0''|$ ) and allows to cool the relative motion to temperatures lower than that of independent atoms,  $\bar{n}_A < \bar{n}_{ind}$ . The symmetric spin state  $|S\rangle$ , however, becomes superradiant ( $\gamma_S > \gamma_0$  and  $|\gamma_S''| > |\gamma_0''|$ ) and the center-of-mass motional mode gets cooled to a temperature higher than that of

independent atoms,  $\bar{n}_S > \bar{n}_{ind}$ . Notably, the phonon number of the center-of-mass motion is additionally increased as the drive is off-resonant with the cooling sideband of the symmetric spin state by  $2J_{12}$ . One can numerically check that no net improvement is gained over non-interacting atoms as  $\bar{n} \equiv (\bar{n}_A + \bar{n}_S)/2 \geq \bar{n}_{ind}$ . This result can be understood from the analytical estimations of  $\bar{n}_S$  and  $\bar{n}_A$ . Neglecting the terms associated to diffusion we obtain

$$\bar{n} = \frac{\bar{n}_A + \bar{n}_S}{2} \simeq \frac{\gamma_A^2 + \gamma_S^2}{32\bar{\nu}^2} + \frac{J_{12}^2}{2\bar{\nu}^2} \geq \frac{\gamma_0^2}{16\bar{\nu}^2} + \frac{J_{12}^2}{2\bar{\nu}^2} > \bar{n}_{ind}. \quad (\text{S10})$$

Similar conclusions are reached for  $\bar{\nu} \ll \gamma_0$ .

## B. Array cooling

In the opposite regime where the trap frequency difference is much larger than the dissipative cooling rates of the system,

$$\delta\nu \gg \frac{2\eta_j^2\Omega^2}{\gamma_A}, \quad (\text{S11})$$

the time-dependent phases  $e^{\pm i(\nu_1 - \nu_2)t}$  in Eq. (1) rapidly oscillate during the cooling process. As a result, the interactions between the motional degrees of freedom of different atoms average out and can be neglected under the rotating wave approximation. Then, the effective master equation becomes diagonal for the individual atoms and the steady state phonon numbers for the individual atoms are obtained from Eq. (17) as

$$\bar{n}_j = \frac{\mathcal{R}_{jj}^+}{\mathcal{R}_{jj}^- - \mathcal{R}_{jj}^+} = \frac{\mathcal{R}_{Aj}^+ + \mathcal{R}_{Sj}^+}{\mathcal{R}_{Aj}^- + \mathcal{R}_{Sj}^- - \mathcal{R}_{Aj}^+ - \mathcal{R}_{Sj}^+}. \quad (\text{S12})$$

If we additionally assume the trap frequency difference to be small compared to the widths of the cooling and heating sidebands,

$$\delta\nu \ll \gamma_A/2, \quad (\text{S13})$$

the rates  $\mathcal{R}_{\lambda j}^\pm \equiv \mathcal{R}_\lambda^\pm$  are independent of the atom  $j$ . In that case, both atoms reach the same steady state phonon number,  $\bar{n} \approx \bar{n}_1 \approx \bar{n}_2$ , which depends on the magnitude of the trap frequency  $\bar{\nu}$ . We distinguish three cases.

- (i) For  $\bar{\nu} \gg \gamma_S \simeq \gamma_0$ , the cooling and heating sidebands associated to the symmetric and antisymmetric spin states are resolved. For drive on resonance with the antisymmetric cooling sideband,  $\Delta \approx -\bar{\nu} - J_{12}$ , the sum of the cooling rates is dominated by the contribution of the antisymmetric (subradiant) spin state,  $\mathcal{R}_A^- + \mathcal{R}_S^- \approx 4\eta^2\Omega^2/\gamma_A + 4\eta^2\Omega^2\gamma_S/(\gamma_S^2 + 16J_{12}^2) \approx 4\eta^2\Omega^2/\gamma_A$ . We distinguish two cases depending on the strength of the dipole shift  $J_{12}$ .

For  $\nu \gg |J_{12}|$ , both spin modes contribute similarly to the heating rate, which reads  $\mathcal{R}_A^+ + \mathcal{R}_S^+ \approx \eta^2\Omega^2(\gamma_A + \gamma_S)/4\nu^2 - \eta^2\Omega^2(\gamma_A'' + \gamma_S'')/\nu^2 \approx 13\eta^2\Omega^2\gamma_0/10\nu^2$ , where we have used the fact that  $\gamma_A + \gamma_S = \gamma_0$  and  $\gamma_A'' + \gamma_S'' = \gamma_0''$ . Then, the steady state phonon number reads

$$\bar{n} \approx \frac{13\gamma_A\gamma_0}{40\bar{\nu}^2} \quad (\text{for } \nu \gg |J_{12}|). \quad (\text{S14})$$

For  $|J_{12}| \gg \bar{\nu}$ , the heating sideband of the antisymmetric spin state is detuned from the driving field by  $2\bar{\nu}$ , whereas the heating sideband of the symmetric spin state and the Lorentzian associated to recoil or diffusion are detuned by  $2\bar{\nu} + 2J_{12} \gg 2\bar{\nu}$  and  $\bar{\nu} + 2J_{12} \gg 2\bar{\nu}$ . As a result, only the heating sideband of the antisymmetric spin state significantly contributes to heating,  $\mathcal{R}_A^+ + \mathcal{R}_S^+ \approx \eta^2\Omega^2\gamma_A/4\nu^2$ , and the steady state phonon number is reduced to

$$\bar{n} \approx \frac{\gamma_A^2}{16\bar{\nu}^2} \quad (\text{for } \bar{\nu} \ll |J_{12}|). \quad (\text{S15})$$

Typically, this regime requires very small separations between the atoms, for which  $J_{12} \gg \gamma_0$ . The transition from Eq. (S14) to Eq. (S15) is showcased in the deviation of the numerically obtained phonon number from Eq. (S14) in Fig. 2(c) for  $\bar{\nu} = 100\gamma_0$ . For smaller values of  $\bar{\nu}$ , this deviation is more significant and appears already at larger spacings  $d$ .

- (ii) For  $\gamma_A \ll \bar{\nu} \lesssim \gamma_0$ , only the sidebands associated to the antisymmetric subradiant spin rate can be resolved (i. e., ground-state cooling cannot be achieved for non-interacting atoms in this regime). As a result, the denominator in Eq. (S12) is still dominated by the contribution of the antisymmetric spin rate,  $\mathcal{R}_A^-$ . Now  $|J_{12}| \geq \gamma_0 \geq \bar{\nu}$  already for moderately small distances  $d \leq \lambda_0/2$ , such that the heating rate is predominantly dictated by the heating sideband of the antisymmetric state. This results again in the steady state phonon number given by Eq. (S15).
- (iii) For  $\bar{\nu} \ll \gamma_A/2 \leq \gamma_0/2$ , the sidebands are not resolved (neither in the interacting nor in the non-interacting case). Again, the cooling and heating sidebands of the antisymmetric state are the dominant rates of the system, since the contribution from the sidebands of the symmetric states and the recoil Lorentzian at subwavelength spacings are off-resonant by  $J_{12} \gtrsim \gamma_0 \gg \bar{\nu}$  and can therefore be neglected. Then, the cooling and heating rates respectively read  $\mathcal{R}_A^- + \mathcal{R}_S^- \approx 2\eta^2\Omega^2/\gamma_A + 4\eta^2\Omega^2\bar{\nu}/\gamma_A^2$  and  $\mathcal{R}_A^+ + \mathcal{R}_S^+ \approx 2\eta^2\Omega^2/\gamma_A - 4\eta^2\Omega^2\bar{\nu}/\gamma_A^2$ , and the atoms reach the steady state phonon number

$$\bar{n} \approx \frac{\gamma_A}{4\bar{\nu}}, \quad (\text{S16})$$

which is larger than one. In other words, ground state-cooling is not possible.

Notably, the steady state phonon number scales with  $\gamma_A$  for all values of  $\bar{\nu}$ , thereby allowing to reach lower phonon numbers than for non-interacting atoms at subwavelength spacings, when  $\gamma_A \ll \gamma_0$ .

### C. Single-atom cooling

As evidenced by Eq. (S2), the cooling and heating rates  $\mathcal{R}_{\lambda_j}^\pm$  associated to different atoms  $j$  differ if the trap frequency difference is larger than the width of the sidebands,

$$\delta\nu \gg \frac{\gamma_A}{2}. \quad (\text{S17})$$

Together with the condition for the adiabatic elimination of the spin degrees of freedom,  $\eta\Omega \ll \gamma_A$ , Eq. (S17) implies that the trap frequency difference is also much larger than the dissipative interactions of the system,  $\mathcal{R}_{12}^- \approx -\mathcal{R}_{A1}^-/4 \approx -\eta^2\Omega^2/\gamma_A$ , as indicated by Eq. (S11). Then, the steady state phonon number is again given by Eq. (S12). From a physical point of view, a single laser drive cannot be simultaneously on resonance with the antisymmetric cooling sideband of both atoms under Eq. (S17). As a result, only one atom can be cooled at a time. If the drive is on resonance with the antisymmetric cooling sideband of atom 1,  $\Delta = -\sqrt{\nu_1^2 + (\gamma_A/2)^2} - J_{12}$ , atom 1 is still cooled to the same steady state phonon number as in the array cooling regime. For atom 2, however, the drive is not on resonance with its antisymmetric cooling sideband, and its steady state phonon number consequently increases. For example, in the resolved regime  $\nu_{1,2} \gg \gamma_0$  and assuming  $\nu_{1,2} \gg |J_{12}|$  and  $\delta\nu \ll \nu_2$ , the cooling rate for atom 2 is reduced to  $\mathcal{R}_{A2}^- + \mathcal{R}_{S2}^- \approx \eta^2\Omega^2\gamma_A/(\gamma_A^2 + 4\delta\nu^2)$  and its steady state phonon number reads

$$\bar{n}_2 \approx \frac{13\gamma_A\gamma_0}{40\nu_2^2} \left( 1 + \frac{4\delta\nu^2}{\gamma_A^2} \right). \quad (\text{S18})$$

That is, the steady state phonon number of atom 2 increases by a factor  $\bar{n}_2/\bar{n}_1 \approx 4\delta\nu^2/\gamma_A^2 \gg 1$ , and typically becomes larger than that of non-interacting atoms. Note that similar arguments hold for the other ranges of  $\bar{\nu}$  discussed in the array cooling section.

## II. DEPENDENCE ON THE TRANSITION DIPOLE MOMENT

In this section, we discuss the dependence of the steady state phonon number attained in the array cooling regime on the direction of atomic polarization. For that, it is instructive to first consider the case of two atoms located at a distance  $d$  along the  $x$ -axis and moving along the  $z$ -direction. The optical response of the system features: (a) two cooling sidebands associated to the antisymmetric and symmetric collective spin modes, respectively centered at  $\Delta = -\nu_1 - J_{12}$  and  $\Delta = -\nu_1 + J_{12}$ ; (b) two heating sidebands associated to the antisymmetric and symmetric collective spin modes, respectively centered at  $\Delta = \nu_1 - J_{12}$  and  $\Delta = \nu_1 + J_{12}$ ; (c) a heating contribution from the

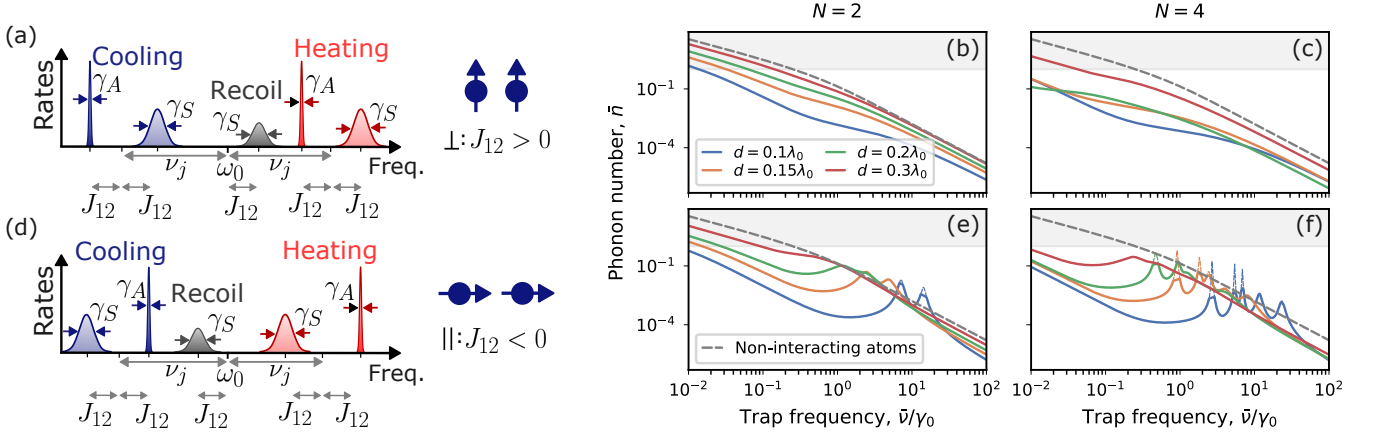


Figure S1. (a) For atoms polarized perpendicular to the axis of the chain, the subradiant antisymmetric spin mode is shifted to negative energies. The antisymmetric cooling sideband moves away from the symmetric heating sidebands and the recoil Lorentzian for decreasing spacing. As a result, the phonon number  $\bar{n}$  remains below that of non-interacting emitters for all  $\bar{\nu}$ , both for (b) chains of 2 atoms and (c) chains of 4 atoms. (d) For atoms polarized in the axis of the chain, the subradiant antisymmetric spin mode is shifted to positive energies. Then, the antisymmetric cooling sideband can become resonant with symmetric heating sidebands and the recoil Lorentzian. As a result, the steady state phonon number  $\bar{n}$  for (e) chains of 2 atoms and (f) chains of 4 atoms can become larger than that of non-interacting atoms for specific combinations of  $\bar{\nu}$  and  $J_{12}$ . The solid lines correspond to a drive on resonance with the cooling sideband of the collective spin mode that leads to a smallest phonon number, whereas the dashed lines correspond to a drive on resonance with the cooling sideband of the darkest spin mode. Notably, when the cooling sideband of the darkest spin mode becomes resonant with either a heating sideband of another spin mode or the recoil Lorentzian, cooling can be enhanced by driving a spin mode with a larger linewidth for which this coalescence does not occur. The results are obtained for  $\eta = 0.02$  and  $\nu_j = \bar{\nu} + \delta\nu(j - \lfloor N/2 \rfloor - 1)$  with  $\bar{\nu} = 20\gamma_0$  and  $\delta\nu = 5 \times 10^{-4}\gamma_0$ .

recoil or diffusive motion in the form a Lorentzian centered at  $\Delta = J_{12}$ . As we have done throughout this work, we consider the drive to be on resonance with the antisymmetric cooling sideband. Then, the symmetric heating sideband and the contribution from recoil are respectively detuned from the driving field by  $\delta_{hs} = 2(\nu_1 + J_{12})$  and  $\delta_r = \nu_1 + 2J_{12}$ . There exist two different scenarios depending on the sign of the coherent dipole-dipole interaction  $J_{12}$  at small inter-atomic distances, which in turn depends on the atomic polarization [Fig. S1(a) and (d)]:

- (i) For polarization perpendicular to the array and the drive (i.e., along  $\mathbf{y}$ ), we obtain  $J_{12} > 0$  for  $d < 0.7\lambda_0$ . Since both the trap frequency  $\nu_j$  and  $J_{12}$  are positive, the detunings  $\delta_{hs}$  and  $\delta_r$  cannot become zero. In other words, the symmetric heating sideband and the heating contribution arising from recoil can never be on resonance with the antisymmetric cooling sideband, as illustrated in Fig. S1(a). As a result, the steady state photon number in the array cooling regime and at small distances  $d$  is always smaller than that of non-interacting atoms, as shown in Fig. S1(b). Note that this is the configuration considered in the main text.
- (ii) For atoms polarized along the direction of the atomic chain (i.e., along  $\mathbf{x}$ ), we obtain  $J_{12} < 0$  for  $d < 0.43\lambda_0$ . As illustrated in Fig. S1(d), it is now possible for the antisymmetric cooling sideband to become on resonance with either the symmetric heating sideband or the recoil Lorentzian. This respectively occurs when  $\nu_1 = -J_{12}$  and  $\nu_1 = -2J_{12}$ , and leads to increased steady state phonon numbers as shown in Fig. S1(e). In particular, the phonon number can become larger than that of non-interacting atoms, such that the cooling advantage arising from the narrow collective resonance is lost. In general, this effect can be minimized by driving on resonance with the cooling sideband associated to another spin mode (in this case, the symmetric cooling sideband), or by separating the atoms by distances such that the different resonances do not overlap for the specific trap frequency considered.

This phenomenon also occurs for larger atom numbers. In Fig. S1(c) and (f), we show an example for a chain of 4 atoms. For perpendicular polarization, the most subradiant spin mode is also associated to the most negative energy shift, and efficient cooling is attained for all spacings and trap frequencies. For polarization along the atomic

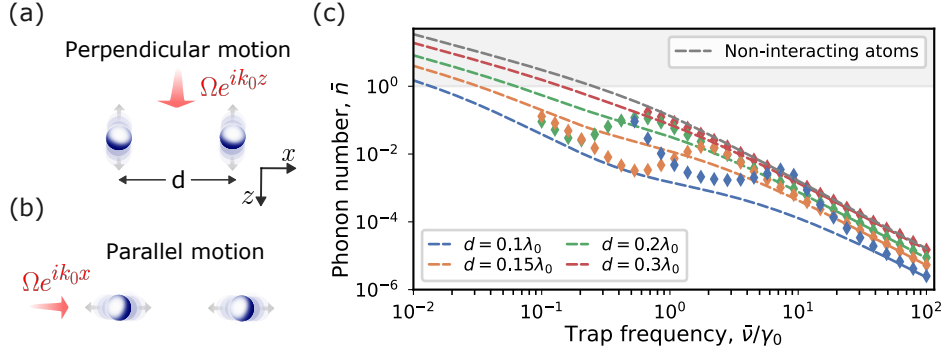


Figure S2. (a) Two trapped atoms at a distance  $d$  along the  $x$ -axis move in the perpendicular direction ( $z$ -axis). The drive is applied along the direction of motion, such that  $\Omega_j = \Omega e^{ik_0 z_j} \equiv \Omega$ . (b) Two trapped atoms at a distance  $d$  along the  $x$ -axis move in the same direction (parallel motion). The drive is applied along the direction of motion, such that  $\Omega_j = \Omega e^{ik_0 x_j}$ . (c) Steady state phonon number per atom  $\bar{n}$  for perpendicular (dashed lines) and parallel (markers) motion, respectively obtained by solving the effective master equation (1) and the full master equation (8) including spin and motion. We consider  $\eta = 0.02$  and  $\delta\nu = 10^{-3}\gamma_0$ .

chain, that is no longer the case and cooling via the most subradiant spin mode leads to phonon numbers larger than that of non-interacting atoms for certain combinations of  $\bar{\nu}$  and  $d$  that lead to coalescence of sidebands. Again, it is generally possible to minimize this extra heating by driving on resonance with the cooling sideband associated to another collective spin mode for which this coalescence does not occur [see the reduced temperature for the solid lines as opposed to the dashed lines in Fig. S1(f)]. Alternatively, there always exists a spacing  $d$  such that the array can be cooled to temperatures lower than that of non-interacting atoms independently of  $\bar{\nu}$ .

### III. DEPENDENCE ON THE AXIS OF ATOMIC MOTION

In the main text, we demonstrate enhanced cooling of interacting chains of atoms located on the  $x$ -axis and moving along the perpendicular direction, that is, along the  $z$ -axis. In this section, we extend the analysis to motion along the atomic chain, i. e., along the  $x$ -axis. For that, we consider the case of two atoms placed at a distance  $d$ . While  $J'_{ij}$  and  $\gamma'_{ij}$  are zero for perpendicular motion, they are non-zero for parallel motion. Then, the coherent spin-motion interaction to first order in  $\eta$  and after applying the displacement transformation to the atomic spins in the low-intensity limit reads

$$\hat{V}_1 = \sum_j \left( \eta_j \Omega'_j \hat{r}_j \hat{\sigma}_j^\dagger + h.c. \right) + \sum_{i,j \neq i} J'_{ij} (\eta_i \hat{r}_i - \eta_j \hat{r}_j) \left( \hat{\sigma}_i^\dagger \hat{\sigma}_j + s_i^{*(0)} \hat{\sigma}_j + s_j^{(0)} \hat{\sigma}_i^\dagger \right). \quad (\text{S19})$$

For drive along the  $x$  direction, the Rabi frequency and its derivative read  $\Omega_j = \Omega e^{ik_0 x_j}$  and  $\Omega'_j = i\Omega_j$ , as illustrated in Fig. S2(b). For drive on resonance with the antisymmetric cooling sideband  $\Delta \approx -\bar{\nu} - J_{12}$ , the spin displacements take the form

$$s_1^{(0)} = -\Omega \frac{\bar{\nu} + J_{12} (1 - e^{ik_0 d}) - i(\gamma_0 + e^{ik_0 d} \gamma_{12}) / 2}{(\bar{\nu} - i\gamma_A/2)(\bar{\nu} + 2J_{12} - i\gamma_S/2)}, \quad (\text{S20})$$

and similarly for  $s_2^{(0)}$ . For  $\bar{\nu} \gg |J_{12}|, |J'_{12}|, \gamma_{12}, \gamma'_{12}$ , the displacement can be approximated to  $s_j^{(0)} \approx -\Omega_j / \bar{\nu}$ . Then, the strength of the spin-motion coupling arising from light-induced dipole-dipole interactions is much smaller than the contribution from the driving field, i. e.,  $\eta_j |J'_{12}| |s_j^{(0)}| \approx \eta_j |\Omega_j| |J'_{12}| / \bar{\nu} \ll \eta_j |\Omega_j|$ , and the steady state phonon number  $\bar{n}$  is identical for parallel and perpendicular motion. This is shown in Fig. S2(c), where we compare  $\bar{n}$  for parallel motion obtained by solving the full master equation (8) including the spin and motional degrees of freedom (markers) with the  $\bar{n}$  for perpendicular motion obtained by solving the effective master equation (1). For  $|J'_{12}| \gtrsim \bar{\nu}$ , the dipole-dipole contribution to the spin-motion interaction can become dominant, and the steady state phonon number for parallel and out-of-plane motion can differ. As shown in Fig. S2(c), this divergence occurs at larger  $\bar{\nu}$  for smaller atomic separations  $d$  as  $|J'_{12}|$  increases. Notably, enhanced cooling is still found for a wide range of trap frequencies  $\bar{\nu}$  and distances  $d$ .



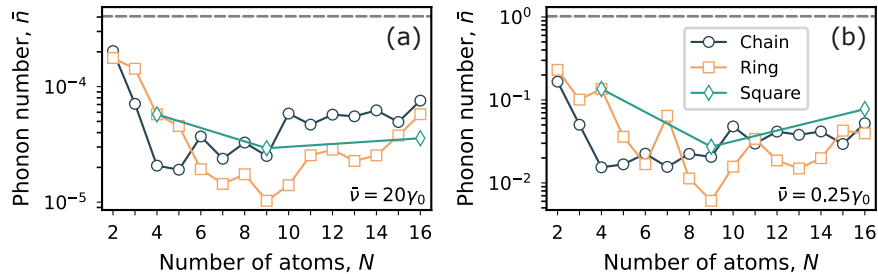


Figure S3. Steady state phonon number  $\bar{n}$  for arrays of different geometries as a function of atom number  $N$ , for (a)  $\bar{\nu} = 20\gamma_0$  and (b)  $\bar{\nu} = 0.25\gamma_0$ . We consider a linear ordered chain, a square two-dimensional lattice and a ring of atoms. The atomic chain is placed along the  $x$ -axis and the atoms are polarized along the  $y$ -direction. In all cases, the atoms move along the  $z$ -direction. The squared array and the ring are placed in the  $xy$ -plane and the atoms are circularly polarized in the  $xy$ -plane. For the atomic chain and the squared array, we consider a lattice spacing  $d = 0.2\lambda_0$ , while the ring has a radius such that neighboring atoms are at a distance  $d = 0.2\lambda_0$ . The results are obtained for  $\eta = 0.02$  and all atoms have different trap frequencies in increments of  $\delta\nu = 5 \times 10^{-4}\gamma_0$ , such that the system is in the array cooling regime.

#### IV. ALTERNATIVE GEOMETRIES

The results presented in the main text for ordered chains of atoms can be readily extended to other geometries, such as two-dimensional squared arrays or rings of atoms. To exemplify this versatility, in Fig. S3 we show the steady state phonon number as a function of atom number  $N$  for  $\bar{\nu} = 20\gamma_0$  and  $\bar{\nu} = 0.25\gamma_0$  and for atoms arranged in chains, rings, and squares. For the system to be in the array cooling regime, we consider different atoms to have different trap frequencies. For the chain and the ring of atoms, we apply a gradient profile  $\nu_j = \bar{\nu} + \delta\nu(j - \lfloor N/2 \rfloor - 1)$ , where  $\lfloor N/2 \rfloor$  denotes the integer value of  $N/2$  rounded down. For the two-dimensional array, the gradient is applied in both directions of the lattice, such that all atoms have different trap frequencies in increments of  $\delta\nu$ . We find enhanced cooling to phonon numbers lower than that of non-interacting atoms for all geometries up to 16 atoms.

#### V. SPEEDING UP COOLING RATES

In this section, we describe the method used to extract the critical cooling rates in the main text and discuss several possibilities to speed up the cooling process.

Let us consider two atoms in the array cooling regime (i.e., the atoms have different trap frequencies, such that the exchange of motional quanta between atoms is suppressed) and the subradiant cooling sideband to be resolved (i.e.,  $\gamma_A \ll \bar{\nu}$ ). The steady state phonon number  $\bar{n}$  and the cooling rate  $\Gamma$  at which it is reached depend on the drive strength. For sufficiently small drive strength, such that the system remains in the array cooling regime  $\Omega^2 \ll \delta\nu\gamma_A/2\eta^2$  and the spin-motion coupling is weak  $\Omega \ll \gamma_A/\eta$  (note that this condition is required to adiabatically eliminate the spin degrees of freedom), the phonon number exponentially decays to its steady state value at a rate  $\Gamma = \mathcal{R}^- - \mathcal{R}^+ \approx \mathcal{R}^- \approx 2\eta^2\Omega^2/\gamma_A$ , as shown in Fig. S4(a) and (b) for  $\bar{\nu} = 20\gamma_0$ . As the drive strength increases, either the array cooling condition or the weak spin-motion coupling condition breaks down, and the effective master equation resulting in Eq. (17) stops being valid. In that case,  $\bar{n}$  and  $\Gamma$  can only be obtained by numerically solving the full system including spin and motional degrees of freedom. More precisely,  $\Gamma$  is obtained by fitting an exponential decay to the phonon number over time, as shown in the inset of Fig. S4(a). We find that, as soon as one of the two conditions is violated, the phonon number starts to increase with increasing  $\Omega$  and the cooling rate eventually decreases. To better understand this process, we plot  $\bar{n}$  as a function of cooling rate in Fig. S4(c). That is, each data point in this plot corresponds to a different value of  $\Omega$ . In the main text, we defined the critical cooling rate  $\Gamma_c$  as the one obtained at the driving strength  $\Omega$  that leads to a steady state phonon number 10% larger than the optimal one. For two atoms at a distance  $d = 0.1\lambda_0$ , this corresponds to the squared marker in Fig. S4(c). However, this condition is more restrictive for lattices with darker spin modes than attain lower phonon numbers. In other words, we could drive the two atoms at a distance  $d = 0.1\lambda_0$  stronger and thereby attain a larger cooling rate while still reaching steady state phonon numbers smaller than in the case of independent atoms,  $\bar{n} < \bar{n}_{ind}$ . This motivates us to introduce an alternative definition for the critical cooling rate  $\Gamma'_c$  as the largest possible rate that can be reached such that the phonon number remains smaller than  $1.1\bar{n}_{ind}$ . As an example,  $\Gamma'_c$  and its corresponding  $\bar{n}'$  are shown

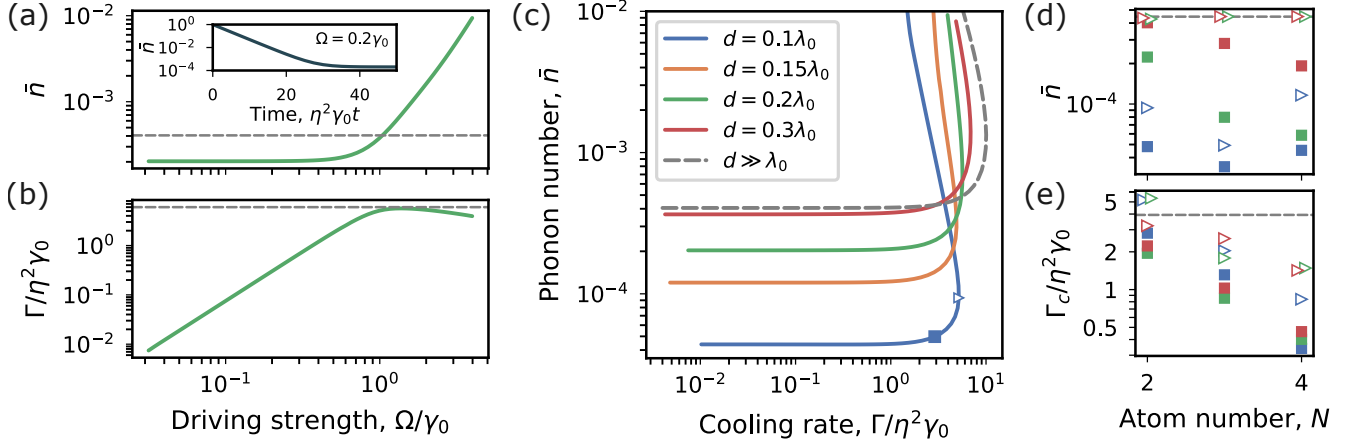


Figure S4. (a) Steady state phonon number  $\bar{n}$  and (b) cooling rate  $\Gamma$  as a function of drive strength  $\Omega$  for two atoms separated by a distance  $d = 0.2\lambda_0$  along the  $x$ -axis, polarized along the  $y$ -axis and moving along the  $z$ -axis. The inset shows an instance of the exponentially decaying phonon number over time for  $\Omega = 0.2\gamma_0$ , from which the cooling rate is fitted. (c) Steady state phonon number versus cooling rate for various spacings. Each point corresponds to a different value of  $\Omega$ . The squared marker corresponds to the critical cooling rate  $\Gamma_c$ , obtained at the drive strength that results in a steady state phonon number 10% larger than the optimal one. The triangular marker corresponds to the alternative critical cooling rate  $\Gamma'_c$ , obtained at the drive that results in a largest cooling rate while maintaining a steady state phonon number smaller than  $1.1\bar{n}_{ind}$ . (d-e) Critical cooling rates  $\Gamma_c$  and  $\Gamma'_c$  and their corresponding steady state phonon numbers for chains of  $N$  atoms and various spacings. In all panels, we consider  $\eta = 0.02$  and  $\nu_j = \bar{\nu} + \delta\nu(j - \lfloor N/2 \rfloor - 1)$  with  $\bar{\nu} = 20\gamma_0$  and  $\delta\nu = 5 \times 10^{-3}\gamma_0$ .

by the triangular marker in Fig. S4(c) for  $d = 0.1\lambda_0$ . In Fig. S4(d) and (e), we plot  $\bar{n}$  and  $\Gamma_c$  for chains of  $N$  atoms with various spacing  $d$  for  $\bar{\nu} = 20\gamma_0$ . Again, squared and triangular markers denote the two different definitions for the critical cooling rate. In all cases,  $\Gamma'_c \gtrsim 2\Gamma_c$ , showing that the critical cooling rates presented in the main text can be sped up by driving the system stronger at the expense of reaching larger steady state phonon numbers  $\bar{n}'$ ; this suggests the following protocol for efficient cooling: first, the system is cooled at  $\Gamma'$  to a phonon number close to  $\bar{n}'$ ; then, the drive is dynamically reduced until the lowest possible phonon number  $\bar{n}$  is eventually reached.

Figure S4(e) also shows that the critical cooling rate decreases with atom number  $N$ . This trend can be understood by examining the cooling rate in Eq. (19) in the adiabatic limit with weak spin-motion coupling. Assuming the spin modes to be mostly delocalized and have an overlap  $\sim 1/\sqrt{N}$  with each atom and, we can approximate the cooling rate associated to atom  $j$  in the resolved sideband regime as

$$\mathcal{R}_{jj}^- \approx \eta_j^2 \Omega^2 \frac{1}{N} \sum_{\lambda} \frac{\gamma_{\lambda}}{(-\Delta + J_{\lambda} - \nu_j)^2 + (\gamma_{\lambda}/2)^2} \approx \sum_{\lambda} \frac{\mathcal{R}_{\lambda j}^-}{N}, \quad (\text{S21})$$

where  $\gamma_{\lambda}$  and  $J_{\lambda}$  are the collective linewidth and frequency shift of the spin mode  $\lambda$ , and  $\mathcal{R}_{\lambda j}^-$  denotes the contribution from each spin mode. Because of the emergence of frequency shifts such that  $|J_{\lambda} - J_{\lambda'}| > \gamma_{\lambda}, \gamma_{\lambda'}$  for narrow spin transitions, a monochromatic driving field can only drive on resonance the sideband of a single subradiant spin mode. That is, out of the  $N$  collective spin states, only one subradiant mode can significantly contribute to the cooling rate in Eq. (S21). Additionally noting that the subradiant decay rates are bounded by  $\sim \eta^2\gamma_0$  in the case of trapped atoms, this results in a decrease of the cooling rate of an atomic array with increasing  $N$ .

Apart from the sequential cooling scheme described in the main text, several alternative schemes can be utilized to circumvent this issue:

- (i) Multiple spin modes can contribute to cooling if one applies multiple driving fields, each at the resonance frequency of the cooling sideband of a different subradiant spin mode. Note that this method also increases the heating rates, and could possibly lead to larger steady state phonon numbers.
- (ii) Engineering of alternative spatial arrangements of atoms can lead to multiple subradiant spin modes having the same resonance frequency.
- (iii) Dynamically modifying the spacing  $d$  of the array can lead to a faster cooling process. For that, one places the atoms at  $d > \lambda_0$  at initial times, such that the cooling process is similar to that of independent atoms (i.e.,

in that case, the spin modes are not collective, simply correspond to the individual atoms and are therefore on resonance). Once the temperature reaches that limit, the spacing can be reduced to finally attain lower phonon numbers at reduced speeds.